Institut für Physikalische Elektronik

Institute of Physical Electronics

Universität Stuttgart

Jahresbericht

Annual Report

2002

Institut für Physikalische Elektronik
Pfaffenwaldring 47
D-70569 Stuttgart
Tel.: +49-711-685-7141
Fax: +49-711-685-7143
http://www.ipe.uni-stuttgart.de

Redaktion/*edited by*:
Uwe Rau
Fritz Pfisterer
Jürgen H. Werner

Inhaltsverzeichnis / *Table of Contents*

1 Vorwort

Liebe Freunde des *ipe*,

seit dem 1.10.2002 haben wir die neue Fakultät Informatik, Elektrotechnik und Informationstechnik. Die Universität Stuttgart mit jetzt nur noch 10 anstatt 14 Fakultäten hat ein neues Gesicht. Die Bündelung von Kräften wird hoffentlich dazu beitragen, unserer Universität auch weiterhin auf Jahre hinaus einen Spitzenplatz unter den Universitäten in Deutschland zu sichern. Schon die frühere Fakultät Elektrotechnik und Informationstechnik hat in der Vergangenheit bei allen Beurteilungen immer einen solchen Spitzenplatz eingenommen, was vor allem an der hohen Zahl eingeworbener Drittmittel lag. Angesichts der Tatsache, dass „unsere Stuttgarter Elektrotechnik" inzwischen nur noch über 12 Professorenstellen verfügt, ist dies eine erstaunliche Tatsache. Pro Professur treiben wir nahezu doppelt so viele Drittmittel ein wie unsere Konkurrenten an anderen Spitzenuniversitäten wie Aachen oder Berlin. Neben dieser hohen Drittmittelzahl ist es besonders erfreulich, dass die Zahl der Anfänger des Studiums „Elektrotechnik und Informationstechnik" in diesem Oktober wieder bis auf 220 gestiegen ist.

Nach über sechs Jahren (seit Juli 1996) an der Universität Stuttgart ist es auch für mich an der Zeit, eine gewisse Bilanz für das *ipe* zu ziehen: In den letzten sechs Jahren (1.1.1997-31.12.2002) haben am *ipe* knapp 30 junge Wissenschaftler und Wissenschaftlerinnen promoviert. Die meisten von ihnen sind nach Abschluß ihrer Promotion in die Industrie gegangen, wo einige bereits nach kurzer Zeit in Leitungsfunktionen aufgestiegen sind. Im gleichen Zeitraum haben etwa 160 Studenten ihre Diplom- oder Studienarbeit am *ipe* abgeschlossen. Bei höchstem wissenschaftlichen Anspruch konnten diese hohen Zahlen nur erreicht werden, weil alle Mitarbeiter des *ipe*, vor allem die Gruppenleiter und unsere Doktoranden, die Studenten mit hohem persönlichen Arbeitseinsatz unterstützt haben. Trotzdem hat unsere Forschung nicht gelitten. Wir haben in den vergangenen sechs Jahren über 250 wissenschaftliche Arbeiten veröffentlicht, ungefähr jeweils zur Hälfte als Originalpublikationen in referierten Zeitschriften und als Beiträge zu internationalen Konferenzen.

Unsere wissenschaftlichen Leistungen des vergangenen Jahres 2002 haben wir in diesem Jahresbericht wieder in der Form von kurzen Berichten zusammengestellt. Anstatt einen aufwändigen, erst zur Mitte des nächsten Jahres erscheinenden Berichtsband herzustellen, setzen wir auch dieses Jahr wieder ganz bewusst auf unsere wissenschaftliche Substanz und auf Aktualität. Genau darin besteht unsere Stärke. Wir wollen uns durch die Qualität, Kreativität und Seriosität unserer Wissenschaft, Lehre und Personalförderung durchsetzen. Ich bin mir sicher, dass diese Strategie richtig ist.

Ende Oktober des Jahres 2002 ist auch die Ära der Bildverarbeitung am *ipe* zu Ende gegangen: *Peter Schwarzmann* geht in den wohlverdienten Ruhestand. Er, als *ipe*-Urgestein (und von mir oft scherzhaft als „hardcore-Elektrotechniker" bezeichnet), hat am *ipe* bereits im Jahr 1964 beim damaligen Direktor Kluge seine Diplomarbeit angefertigt, war dann in verschiedenen Funktionen unter meinem Vorgänger Bloss weiterhin hier am Institut tätig und hat bis vor kurzem die Gruppe Bildverarbeitung geleitet. In Namen aller Mitarbeiter des *ipe* möchte ich mich bei Dipl.-Ing. Schwarzmann für seine in 38 Jahren stets in höchstem Masse wissenschaftlich kompetente, absolut loyale, aufrichtige, freundliche und sehr erfolgreiche Arbeit bedanken. Ich persönlich habe die Diskussionen und die Zusammenarbeit mit ihm immer sehr genossen und ziehe meinen Hut vor seiner Leistung als Wissenschaftler und als Mensch.

Für das Jahr 2003 wünsche ich allen Mitarbeitern und Freunden des *ipe* ein erfolgreiches berufliches und persönliches Vorankommen. Ich danke allen Mitarbeitern und Mitarbeiterinnen des *ipe* für die mit hohem Einsatz (und weit über den BAT hinaus) erbrachten wissenschaftlichen und technischen Leistungen. Es macht Spass, ein solches Institut zu leiten!

Stuttgart, Dezember 2002

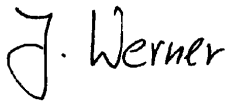

Jürgen H. Werner

Preface

Dear friends of the *ipe*,

Since October 1st, the University of Stuttgart has integrated 14 former faculties into 10 new ones and our institute is now part of the new faculty „*Computer Science, Electrical Engineering and Information Technology*". Hopefully this bundling of strength will contribute to guarantee the excellent position of our University among the best ones in Germany also for the future. Up to now the former faculty "Electrical Engineering and Information Technology" kept a top position, mainly because of our high figure of third-party fundraising. This accomplishment is astonishing, considering the fact that our Electrical Engineering in Stuttgart only disposes of 12 professor positions. The third-party-funds raised per professorship are thus twice as much as in other German top universities like Aachen or Berlin. Another important good news is the fact that the number of new students enrolled for Electrical Engineering and Information Technology has increased up to 220 in October.

After more than six years at the University of Stuttgart (since July 1996) it's time for me to strike a balance of my time at the *ipe*. Between 1997 and 2002 almost 30 young scientist graduated with a PhD-degree. Most of them accepted jobs with the industry, some of them finding themselves already in leading positions. During the same period, nearly 160 students wrote seminar papers and diploma theses at the *ipe*. Keeping in mind our goal of highest scientific standards, this high number could only be achieved by the commitment of our whole staff, especially mentioning our team leaders who assisted their students and dedicated them all the time they needed. The research level also could be maintained: During the last six years, we have published more than 250 scientific papers, about one half as original publications in peer reviewed international journals and the other half as contributions to international conferences.

Our achievements in the year 2002 have been compiled here as short reports. Instead of delivering an elaborate (and expensive) issue in the middle of the coming year, we deliberately focused on scientific substance and timeliness. This seems to be our strength, though. We want to assert ourselves through quality, creativity and reliability of our

research, our teaching and staff promotion. I am convinced that this is the proper strategy for our institute.

The period of Image Processing at the *ipe* has come to an end in October 2002 since Peter Schwarzmann has retired. Being an *ipe*-long lasting colleague (Sometimes a called him a "hardcore-electrical engineer"), he started his career writing his diploma thesis 1964 under the supervision of the then-director Kluge. Later he worked under my predecessor Bloss within different positions and was leading the team Image Processing until quite recently. In the name of the whole *ipe*-staff I would like to thank Mr. Schwarzmann for his 38 years of high quality research, his efficient and successful work. I have always enjoyed the discussions and the co-operation with him, and I admire his achievements as a scientist and appreciate him very much as a person.

I wish the whole *ipe*-staff and the friends of our institute all the best for the coming year 2003, further successful research and personal achievements. Thank you for your high commitment and for all you have accomplished during this year. I appreciate very much being the head of such an institute.

Stuttgart, December 2002

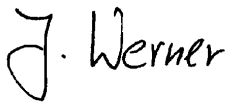

Jürgen H. Werner

2 Lehre am *ipe*

2.1 Vorlesung *Bauelemente der Mikroelektronik I*

Einführung: Informationen; Lehrbuch; Kontakt; das Institut für Physikalische Elektronik; Geschichte der Mikroelektronik; Mikroelektronik heute.
Grundlegende Eigenschaften von Halbleitern: Spezifischer Widerstand; Energiebänder; Messung der Bandlücke; Silicium für die Mikroelektronik; Dotieren von Silicium; das Loch als Quasiteilchen; Energien von Elektronen und Löchern; effektive Massen m*; Leitfähigkeit σ; Konzentration von Ladungsträgern in den Bänden; Elektronen- und Löcherströme; Nichtgleichgewichtszustände.
Elektrostatik des pn-Übergangs: Raumladungszone, Kapazität.
Ströme im pn-Übergang: Minoritätsträgerinjektion; Strom/Spannungskennline; Kleinsignalverhalten.
Spezielle Halbleiterdioden: Photodioden, Solarzellen, Leuchtdioden, Halbleiterlaser.

2.2 Vorlesung *Festkörperelektronik*

Das freie Elektron als Teilchen und als Welle: Teilcheneigenschaften; Welleneigenschaften, Bragg-Bedingung, de-Broglie-Beziehung; Strukturanalyse, LEED.
Die Schrödinger-Gleichung und einige Anwendungen für das freie Elektron: Statistische Deutung der de-Broglie-Wellen, Elektronen in Potentialtöpfen und im Potentialgitter, Fermiverteilung.
Elektronische Bänder in Festkörpern: Reziprokes Gitter, Elektronen im periodischen Potential (Blochwellen, Kronig-Penney-Modell, bewegte Elektronen), effektive Masse, Bandstrukturen wichtiger Halbleiter, Bändermodell, Lochkonzept.
Halbleiter im Bändermodell: Isolatoren, Halbleiter, Metalle; Besetzung der Bänder; elektrostatisches Potential des Halbleiters; Fermi-Niveau im Gleichgewicht.
Ströme in Halbleitern: Feldstrom und Diffusionsstrom, Gesamtstrom, Ströme und Gradienten der Quasi-Fermi-Niveaus.
Austritt von Elektronen aus Metallen und Halbleitern: Austrittsarbeit, thermische Emission, Feldemission (Feldelektronenmikroskop, Rastertunnelmikroskop), Photoemission (äußerer Photoeffekt), Sekundärelektronen-Emission (Rasterelektronenmikroskop).
Der Schottky-Kontakt: Barrierenbildung, Ausbildung der Raumladungszone; Bändermodell; Anlegen von Spannungen, Kennlinie, Bestimmung der Schottky-Barriere, Ohmsche Kontakte.

2.3 Vorlesung *Optoelectronic Devices and Circuits I* (englisch gehalten / *in English*)

Introduction – What is optoelectronics? Overlap of optoelectronics with classic areas; optical regime; scheme of an optical communication system; what is light?

Basic Physics: Simple equations: reflectance, absorbance, transmittance; refraction and total internal reflection; reflectance r_Φ, transmittance t_Φ for $\Theta_i = 0$.

Thermal Radiation: Black body radiation (Kirchhoff's radiation law, Planck's radiation law, Wien's displacement law, Stefan-Boltzmann law); grey body radiation; selective body radiation of a semiconductor.

Coherence: Definition; length of a wavetrain; the frequency spectrum of a wavetrain.

Semiconductor Basics: Energy bands and Fermi function (the wave vector k, the band structure $E(k)$, limited range of k-values, the Brillouin zone, crystal momentum p_k, impulse p_e, direct and indirect bandgap semiconductors).

Excitation and Recombination Processes in Semiconductors: Introduction – What is luminescence? Absorption of radiation in semiconductors; carrier recombination in semiconductors.

Light emitting diodes: Working principle; the emitted spectrum of an LED; materials for LEDs (and lasers); emission efficiency of LEDs.

Semiconductor Lasers: Working principle; laser components; ratio of induced (stimulated) to spontaneous emission; gain of a laser (first general laser condition); the resonator (second general lasing condition); first lasing condition for semiconductor lasers; second lasing condition for a semiconductor laser; heterojunctions, heterostructures; light guiding in semiconductor lasers; stripe contact laser; laser modes; the gain in a semiconductor laser; modern semiconductor lasers.

Glass Fibres: Advantages of glass fibers; fiber configurations; step-index fibers; graded-index fibres; mono-mode fibers; dispersion in glass fibers; attenuation in glass fibers.

Photodetectors: Introduction, general considerations; properties and specifications of photodetectors; photoconductors; photodiodes; photodiodes with internal gain: avalanche photodiodes (APDs); materials and detector configurations.

2.4 Vorlesung *Photovoltaics* (englisch gehalten / *in English*)

Energy Data: Energy units and energy content; consumption of Germany (1995); carbon dioxide creation; mean power for a German.

The Solar Spectrum: The sun as a black body; terrestrial solar spectrum.

Potential of Solar Radiation: Theoretical potential; technical potential of solar energy world wide; technical potential of solar energy in Germany.

The Principal Functions of Photovoltaic Systems .

Generation and Recombination in Semiconductors : Absorption of radiation in semiconductors; recombination.

Basic Semiconductor Equations: Currents in semiconductors; generation and recombination; Haynes-Shockley experiment.

Pn-Junctions: The pn-junction in thermal equilibrium; pn-junction under applied bias.

Current/Voltage-Curve of Solar Cells: Characteristic values of ideal solar cell; equivalent circuit of ideal solar cell; equivalent circuit of real solar cell; characteristic data of real solar cell.

Maximum Efficiency of Solar Cells: Experimental limits; loss processes; radiative efficiency limit after Shockley & Queisser; boundary conditions and a long-standing dogma in PV.

Preparation of Crystalline Silicon: Single crystalline silicon wafers; fabrication of wafers.

Technology of Crystalline Silicon Solar Cells: Screen printing technology; high-efficiency technology.

Amorphous Silicon Solar Cells: Why thin-film solar cells; material properties of amorphous silicon; the Staebler-Wronski effect; structure of an a-Si:H solar cell; preparation of a-Si:H solar cells; module and cell efficiencies; products you can buy.

Cu(In,Ga)Se_2 Solar Cells: Material properties of Cu(In,Ga)Se_2; structure of ZnO/CdS/Cu(In,Ga)Se_2 heterojunction solar cell; variation of the composition of Cu(In,Ga)$(S,Se)_2$ (alloying); preparation of Cu(In,Ga)Se_2 solar cells; cell and module efficiencies; new developments.

2.5 Vorlesung *Energiewandlung*

Einführung: Energieformen, Energieeinheiten; Energiewandlungsprozesse; Energieträger und Ressourcen, Energieverbrauch und Nutzungsarten; Umweltprobleme.

Physikalische Grundlagen: Phänomenologische Thermodynamik (Zustandsgrößen und Zustandsänderungen, Hauptsätze, Kreisprozesse, technische Prozesse); Kernphysik (Kernspaltung, Kernfusion).

Regenerative Energiequellen: Grundlagen (Sonnenspektrum, Planckscher Strahler, Einstrahlungsbedingungen, Konzentration), direkte Nutzung der Sonnenenergie (Solarthermie mit Nieder- und Hochtemperaturprozessen, Photovoltaik mit Lichtabsorption, Materialauswahl, Solarzellenaufbau und Technik photovoltaischer Systeme), indirekte Nutzung der Sonnenenergie (Wasserkraft, Windenergie).

Chemische Speicherung elektrischer Energie: Wasserstofftechnik (Elektrolyse, Wasserstoff-Kreislauf), Methanol als Energieträger (Synthese aus CO_2, Energiebilanz), Brennstoffzellen (Elektrochemische Grundlagen, Energiebilanz, Bauformen wie PAFC, MCFC, SOFC, PEMFC, DMFC, Anwendung im Fahrzeug und in Blockheizkraftwerken), Batterien (Bleiakkumulator, Natrium-Schwefel- und Natrium-Nickelchlorid-Batterie, Zink-Luft-Batterie, Nickel-Metallhydrid-Akku, Lithium-Batteriesysteme).

2.6 Vorlesung *Lasers and Light Sources* (englisch gehalten / *in English*)

The Human Eye: Anatomy of the human eye; rerfracting power D of the human eye; near point, far point; focusing problems; rods, cones; color vision; color deficiency.

Light and Color: Light sensitivity of the human eye; CIE color matching functions^; color coordinates X, Y, Z and color chromaticity coordinates x, y, z; chromaticity diagram; colcor mixing.

Photometry and Colorimetry: Energetic quantities of radiation and irradiation; visual quantities of light and illumination.

Incoherent Light Sources: Black body radiation; gray body radiation; selective body radiation of a semiconductor; emissivity of non-black bodies; incandescent lamps; gas discharge light sources.

Light Emitting Diodes: Working principle; the emitted spectrum of an LED; materials for LEDs (and lasers); emission efficiency of LEDs; organic light emitting diodes (OLEDs).

Lasers: Fundamental processes; occupation probability in thermodynamic equilibrium; microscopic analysis; set-up of a laser; optical resonator; line width; laser types; semiconductor lasers.

2.7 Vorlesung *Thin Film Characterization Methods* (PD Dr. R. B. Bergmann) (englisch gehalten / *in English*)

Introduction: Current questions, problems and challenges of semiconductor characterization; structural, electrical and optical material characterization in the semiconductor industry.

Structural Characterization: Characterization of the semiconductor volume: optical microscopy, (transmission) electron microscopy, defect etching, X-ray diffraction techniques; characterization of semiconductor surfaces: surface reconstruction, surface electron diffraction methods (RHEED, LEED), atomic force microscopy (AFM).

Electrical Characterization: Measurement of majority carrier properties: two and four point probe measurement, spreading resistance, hot probe, Hall-Effect, capacitance-voltage measurements (CV), Deep Level Transient Spectroscopy (DLTS); measurement of minority carrier properties: recombination rate after Shockley-Read-Hall theory, static methods (photoconductivity, quantum efficiency), dynamic methods (carrier decay, current transients).

Optical Characterization: Optical absorption and emission in semiconductors; transmission and reflection measurements, ellipsometry, photoluminescence, Raman spectroscopy.

2.8 Praktika:

Grundlagenpraktikum *Physikalische Elektronik* : im Vorstudium, WS + SS

5 Versuche: LED, Thermoelektrik, Farbfernsehtechnik, Digitale Bildverarbeitung, Photovoltaik und Netzeinspeisung.

Praktikum *Elektrophysik* : im Hauptstudium, SS

a) Praktikum Photovoltaik (mit Inst. f. Plasmaforschung):

8 Versuche: Dünnschichtsolarzellen aus Verbindungshalbleitern, Teil 1: Solarzellenpräparation / Aufdampfanlage;
Dünnschichtsolarzellen aus Verbindungshalbleitern, Teil 2: Absorbercharakterisierung / REM mit EDX;
Elektrische Charakterisierung von Dünnschichtsolarzellen (CIS); Strom-Spannungs-Kennlinie; Bestimmung der Bandlücke E_g, spektrale Quantenausbeute;
Dünnschichtsolarzellen aus amorphem Silicium, Solarzellenpräparation / CVD;
Jahresenergieerträge verschiedener PV-Technologien in Europa, η(E)-Messungen an mono-c-Si-, multi-c-Si-, a-Si- und CIS-Zellen, Berechnung der Jahresenergieerträge für die Standard-Europa-Einstrahlungsverteilung;
Verschaltung von Zellen zu Modulen, Abschattungsprobleme, Bypass- und Blockierdioden;
Inselsystem, Solar Home System, Aufbau und Funktionstest mit SHS-Tester, Simulationsprogramm;
Versuch zur Plasmatechnik am Institut für Plasmaforschung.

b) Praktikum Mikroelektronik (mit Institut für Mikroelektronik Stuttgart):

8 Versuche: Bauelementesimulation mit Atlas (Silvaco), device-Simulation el. Parameter, Diffusion / Oxidation;
Ionenimplantation / Ionen-Projektionslithographie;
Lithographie;
Vakuumtechnik / Aufdampfen;
Materialcharakterisierung / REM / EDX / EBIC;
Schaltungssimulation mit SPICE;
elektr. Charakterisierung / IV / CV ..;
IC-Lab (digitaler Schaltungsentwurf, Hierarchie, Netzlisten, Verifikation).

3 Menschen am *ipe* / *People at the ipe*

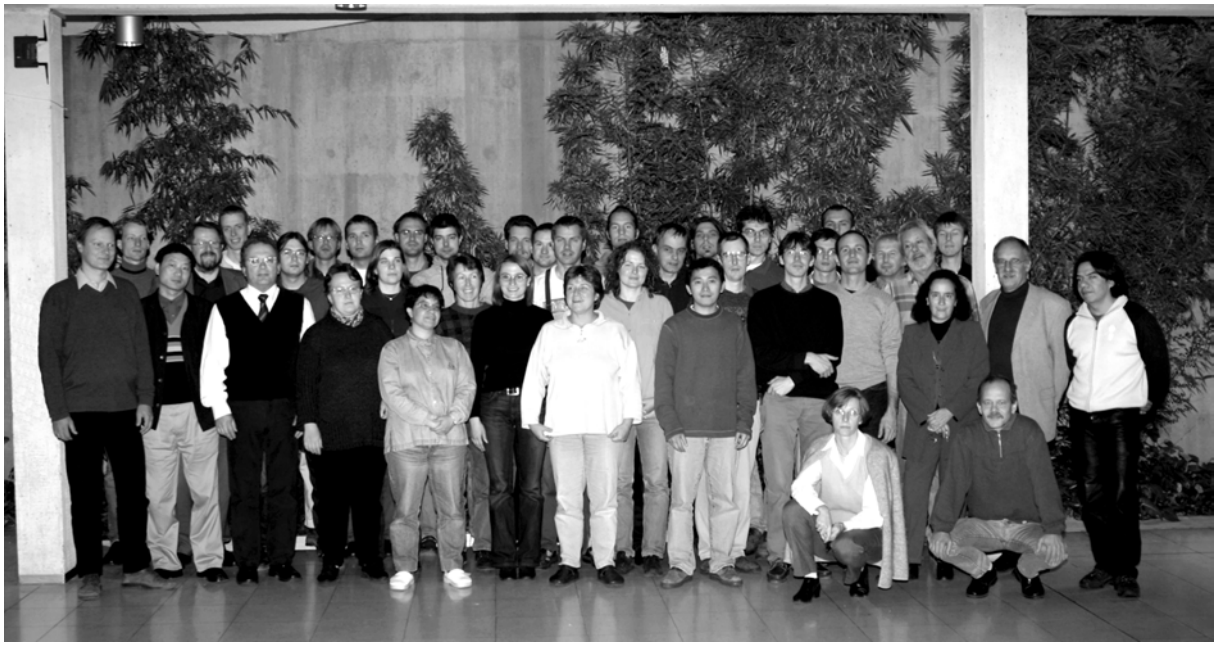

3.1 Verwaltung, Werkstatt und Institutsleitung / *Administration, Workshop, and Head of the Institute*

Verwaltung, Werkstatt und Institutsleitung / *Administration, Workshop, and Head of the Institute:*
Von links *(from left)* : Jürgen Köhler, Christine von Rekowski, Markus Schubert, Jürgen Werner, Fritz Pfisterer, Isabel Kessler, Anton Riß, Lydia Diegel, Werner Wille.

3.2 Gruppe Silicium / *Group Silicon*

Gruppenleiter/Group Leader: MARKUS SCHUBERT
Mitarbeiter/Collaborators: Lukas Alberts, Christopher Berge, Willi Brendle, Klaus Brenner, Anne Carlsson, Cecilia Craff Castillo, Christian Gemmer, Christiane Köhler, Brigitte Lutz, Michail Rakhlin, Martin Rojahn, Thomas Wagner, Maoxiang Yi

Die Arbeitsgruppe "Silicium" des *ipe* entwickelt elektronische Bauelemente auf der Basis von Silicium. Da wir hierzu vorwiegend dünne Schichten verwenden, können Solarzellen, Sensoren und andere Bauelemente direkt auf flexiblen Trägermaterialien hergestellt oder auf biegsame Folien transferiert werden. Wir arbeiten mit allen Modifikationen des Siliciums von einkristallinen Wafern und Dünnschichten bis hin zu nanokristallinen und amorphen Filmen. Unsere Forschungs- und Entwicklungsprojekte konzentrieren sich auf die Anwendung dünner Halbleiterschichten in Solarzellen. Die "integrierte Photovoltaik" (*ipv*) nutzt die mechanische Flexibilität der Dünnschichtzellen, um sie in Kleidung zu integrieren und damit die elektrische Energie zum Betrieb mobiler Kleingeräte bereit zu stellen. In Kooperation mit dem Institut für Mikroelektronik Stuttgart (ims-chips) bietet das Praktikum "Device and Microchip Technologies" Einblick in das Design und die Herstellung moderner Mikroelektronik-Bauelemente. Wafertechnologie und Dünnschichttechnik unterstützen und befruchten sich gegenseitig, beispielsweise in der Entwicklung von "Thin-Film-on-CMOS"-Kameras, Positions- und Thermosensoren.

The silicon group at ipe develops electronic devices based on silicon. We predominantly use thin films. Hence, solar cells, sensors and other devices can directly be deposited onto flexible substrates, or later transferred to bendable foils. We employ all modifications of silicon, from single-crystalline wafers and thin films to nanocrystalline as well as amorphous material. Our main activities in research and development aim at making the best use of thin films for photovoltaic applications. "Integrated Photovoltaics" (ipv) utilizes the mechanical flexibility of our thin film solar cells for integrating them with clothes and accessoires to provide electric power for mobile communication and entertainment electronics. Cooperating with the Institute of Microelectronics Stuttgart (ims-chips), we offer a practical training in "Device and Microchip Technologies" which gives insight into design and manufacturing of modern microelectronic devices. Wafer-based technology and thin film processing mutually enhance each other, e.g. in developing "Thin-Film-on-CMOS" cameras, position and thermosensors.

Gruppe Silicium / *Group Silicon:* Von links *(from left)* : Maoxiang Yi, Christian Gemmer, Christiane Köhler, Martin Rojahn, Cecilia Graff Castillo, Markus Schubert, Christopher Berge, Anne Carlsson, Willi Brendle, Brigitte Lutz, Klaus Brenner (nicht abgebildet / *not present*: Lukas Alberts, Michail Rakhlin, Thomas Wagner).

Beschickung einer Plasma-Depositionsanlage zur Herstellung dünner Schichten aus amorphem Silicium für Solarzellen und Sensoren.

Loading of substrates into a deposition system for plasma enhanced chemical vapour deposition (PECVD) of amorphous silicon layers for solar cells and sensors.

3.3 Gruppe Verbindungshalbleiterschichten / *Group Compound Semiconductor Films*

Gruppenleiter/Group Leader: HANS-WERNER SCHOCK
Mitarbeiter/Collaborators: Kerstin Gebhardt, George Ha nna, Kay Orgassa, Nguyen Hong Quang, Thomas Schlenker, Uli Stempfle, Martin Wagner, Holm Wiesner.

Die Gruppe *Verbindungshalbleiterschichten* entwickelt vor allem Dünnschichtsolarzellen mit Heterostrukturen aus ternären Halbleiterverbindungen wie $CuInSe_2$ (CIS) und verwandten Materialien als Absorberschichten und ZnO als Fensterschicht. Herstellungsverfahren für die Dünnschichten sind eigens hierfür entwickelte Aufdampf- und Sputterprozesse, sowie Abscheidungen aus chemischen Lösungen. Hilfsmittel zur Analyse der Schichten und der Heterostrukturen sind Photoelektronenspektroskopie, Rasterelektronen- und Rasterkraft-mikroskopie sowie Röntgenspektroskopie und Röntgenbeugung. Entwicklungsziele sind die Steigerung der Effizienz der Solarzellen auf 20%, die Weiterentwicklung von Solarzellen aus Verbindungen mit Bandabständen größer als 1,3 eV und entsprechend hoher Leerlaufspannung, die Optimierung von Cd-freien Frontelektroden und darüber hinaus strahlungsbeständige Dünnschichtsolarzellen mit geringem Gewicht für die Raumfahrt. Forschungsthemen sind die generellen Eigenschaften von komplexen Verbindungshalbleitern, insbesondere die Zusammenhänge zwischen Eigendefekten, Verunreinigungen und elektrischen und optischen Eigenschaften.

The *Compound Semiconductor Films* group mainly investigates thin-film solar cells based on ternary compound semiconductors such as $CuInSe_2$ and related compounds. For the deposition of thin films, special coevaporation and sputtering processes as well as chemical processes are designed. Main tools for the optimization of heterostructures are photoelectron spectroscopy, scanning electron microscopy, atomic force microscopy as well as X-ray spectroscopy and X-ray diffraction. Goals of the developments are solar cells with an efficiency of about 20 %, the improvement of solar cells with band gaps in excess of 1.3 eV for high-voltage cells, the optimization of Cd-free front electrodes and, furthermore, radiation resistant, lightweight solar cells for space applications. Topics for research are the general properties of complex compound semiconductors, in particular the relations between native defects, impurities, and the electrical and optical properties.

Gruppe Verbindungshalbleiterschichten / *Group Compound Film Semiconductors:* Von links *(from left)* : Nguyen Quang, Hans-Werner Schock, Thomas Schlenker, George Hanna, Kerstin Gebhardt, Holm Wiesner, Martin Wagner, Kay Orgassa, Uli Stempfle.

Untersuchung von Wachstumsvorgängen dünner Schichten mit dem hochauflösenden Rasterelektronenmikroskop.

Investigation of growth of thin films with a high-resolution scanning electron microscope.

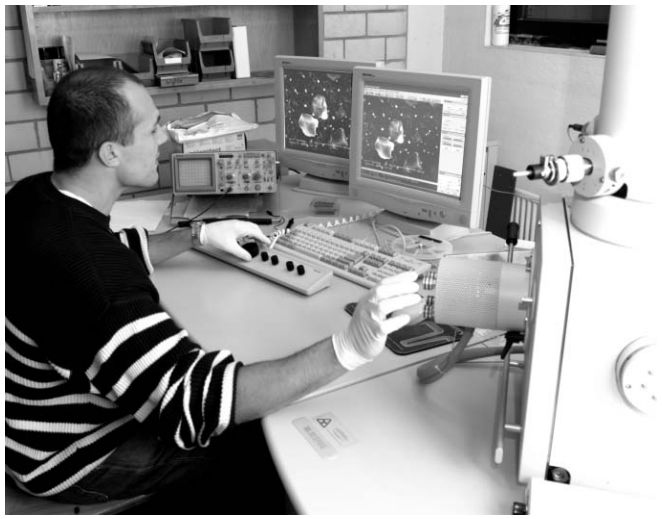

3.5 Gruppe Laserprozesse / *Group Laser Processing*

Gruppenleiter/Group Leader: Jürgen R. Köhler
Mitarbeiter/Collaborators: Ainhoa Esturo-Breton, Jakob Demir

Die Gruppe *Laserprozesse* entwickelt neue Technologien zur Laserprozessierung der am *ipe* verwendeten einkristallinen und polykristallinen Halbleiter. Hierzu zählen die Strukturierung der Halbleiter, deren Kristallisation und Rekristallisation sowie die Laser-Dotierung zur Herstellung von Emittern für einkristalline Silicium-Solarzellen. Im Vordergrund unserer Arbeiten stehen z. Zt. Grundlagenuntersuchungen zur Laserdotierung von einkristallinem Silicium. Ein weiterer Schwerpunkt ist die Laserkristallisation amorpher Siliciumschichten auf Glassubstraten. Diese werden nach der Laserkristallisation zur Herstellung von Dünnfilmtransistoren verwendet, welche ihre Anwendung als Halbleiterbauelemente, sowohl in Aktiv-Matrix adressierten Flüssigkristall-Bildschirmen, als auch in selbstleuchtenden Bildschirmen auf der Basis organischer Leuchtdioden finden. Im Rahmen einer internationalen Kooperation ist es uns gelungen, die in den letzten Jahren etablierte Technologie unter Verwendung von Festkörperlasern weiter zu verbessern. Einen weiteren Schwerpunkt bildet die Charakterisierung polykristalliner Siliciumschichten. In Zusammenarbeit mit der Universität Erlangen konnten wir nachweisen, daß sich die Textur der polykristallinen Silicium-Schicht durch die Silicium-Schichtdicke, die verwendete Pufferschicht und die Pulsfrequenz des Lasers definiert einstellen läßt.

The *laser processing* group explores new technologies for laser processing of monocrystalline and polycrystalline semiconductors. Examples are laser structuring, laser annealing, laser crystallization and laser doping of monocrystalline silicon. During this year we put the main emphasis of our research work on the investigation of a pulsed laser doping process for the preparation of n^+-doped emitters on monocrystalline silicon. Laser crystallization of thin-film silicon on glass is another important application. Our laser-crystallized polycrystalline silicon films are used for the fabrication of thin-film transistors, with possible applications in active matrix liquid crystal displays and displays based on organic light emitting diodes. We characterize our polycrystalline silicon films in collaboration with the University of Erlangen. As one result, we proved a strong dependence of the surface texture of the polycrystalline silicon films, which can be controlled by the silicon layer thickness, the buffer layer material, and the repetition frequency of the laser pulses.

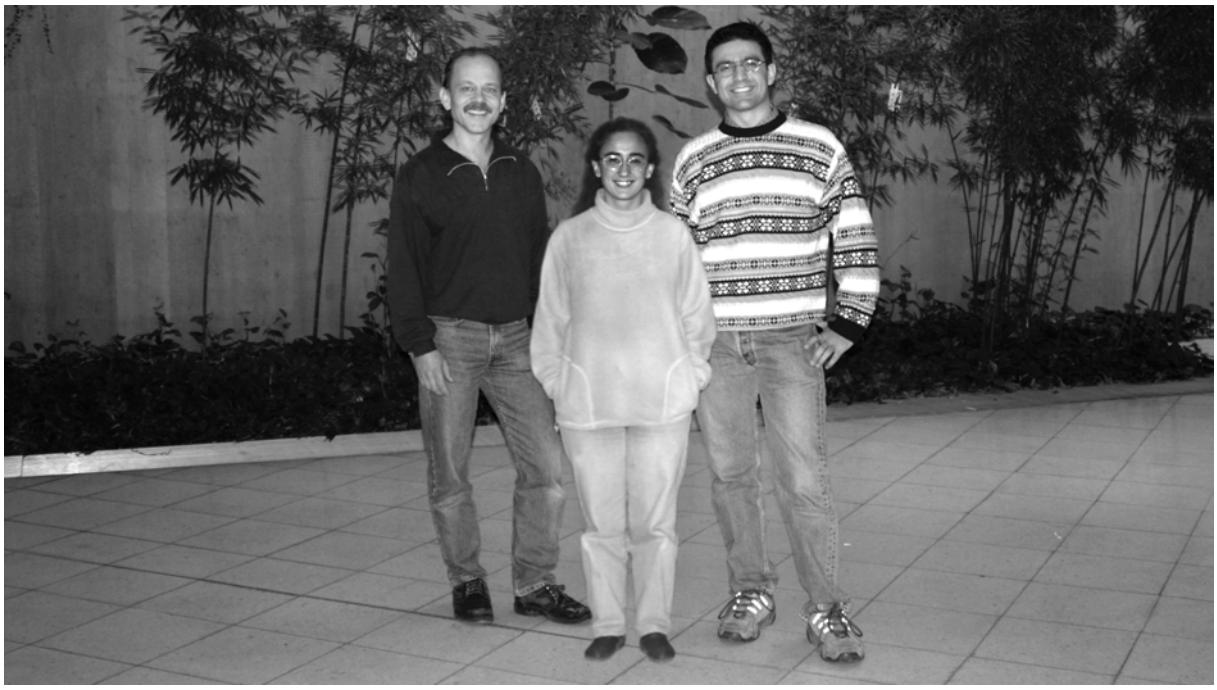

Gruppe Laserprozesse / *Group Laser Processing :*
Von links *(from left)* : Jürgen Köhler, Ainhoa Esturo-Breton, Jakob Demir.

Einbau einer Probe zur anschließenden Laser-Prozessierung.

Fitting of a sample for subsequent laser-processing.

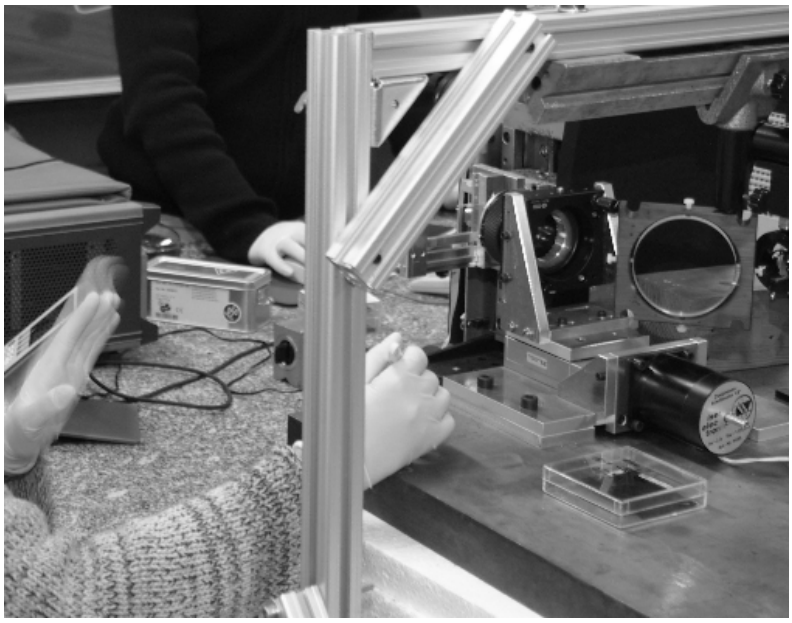

3.6 Gruppe CIS-Technologie und Oberflächenanalyse / *Group CIS Technology and Surface Analysis*

Gruppenleiter/Groupleader: GERHARD BILGER
Mitarbeiter/Collaborators: Leo Bauer, Thomas Dolch, Peter Grabitz, Denis Kühnle, Viktor Laptev

Die bei der *Oberflächenanalyse* angewandten Methoden sind die Sekundärionen-Massenspektrometrie (SIMS) sowie die Röntgen- und Ultraviolett-Photoelektronen-Spektrometrie (XPS, UPS). Die Analytik unterstützt die Gruppen, die Forschung und Entwicklung an Materialien für die Photovoltaik und Sensorik am *ipe* betreiben. Nach außen werden diese Analytikmethoden als Dienstleistungen für die Industrie und andere Institute angeboten. Als sehr empfindliche Methode weist SIMS alle Elemente und deren Verbindungen bis in den ppb-Bereich nach. Tiefen- und ortsaufgelöste Analysen zeigen den Verlauf von Elementverteilungen in einer Schichtfolge und/oder deren laterale Verteilung. XPS-Analysen, empfindlich bis in den 0,1 Atom%-Bereich, sind quantitativ und geben Auskunft über Bindungszustände der Elemente. Die extrem oberflächensensitive Methode weist noch Oberflächenbedeckungen von 1/10 einer Monolage nach. Mit UPS wird die Valenzbandstruktur von Festkörpern untersucht. Bei der *CIS Technologie* liegt die Verantwortung für die Durchführung routinemäßiger Schichtpräparationen und den Unterhalt der dafür notwendigen Infrastruktur.

For *Surface Analysis* the methods applied are Secondary Ion Mass Spectrometry (SIMS), X-ray- and Ultraviolet-Photoelectron Spectrometry (XPS, UPS). These methods support the work of the groups at the Institute of Physical Electronics involved in research and development of materials for photovoltaics and sensors. Analyses are also offered as a service to other institutes and to industry as well. The method SIMS is very sensitive to the detection of all elements and their compositions with concentrations down to the ppb region. SIMS detects the distribution of elements in layers laterally resolved and/or in their depth. The analysis technique XPS is quantitative down to a concentration of 0.1 atomic % and gives information about the chemical binding state. XPS detects surface coverages down to 1/10 of a monolayer. The method UPS is applied to study the structure of the valence band in solids. *CIS Technology* includes the routine preparation of $CuInSe_2$ thin films for solar cells and the maintenance of the infra structure necessary for it.

Gruppe CIS Technologie und Oberflächenanalyse / *Group CIS Technology and Surface Analysis:*
Von links *(from left)* : Leo Bauer, Dennis Kühnle, Viktor Laptev, Peter Grabitz, Uli Stempfle, Gerhard Bilger, Thomas Dolch

Probenpositionierung mit dem Manipulator im Sekundärionen-Massenspektrometer.

Positioning of samples for secondary ion mass analysis.

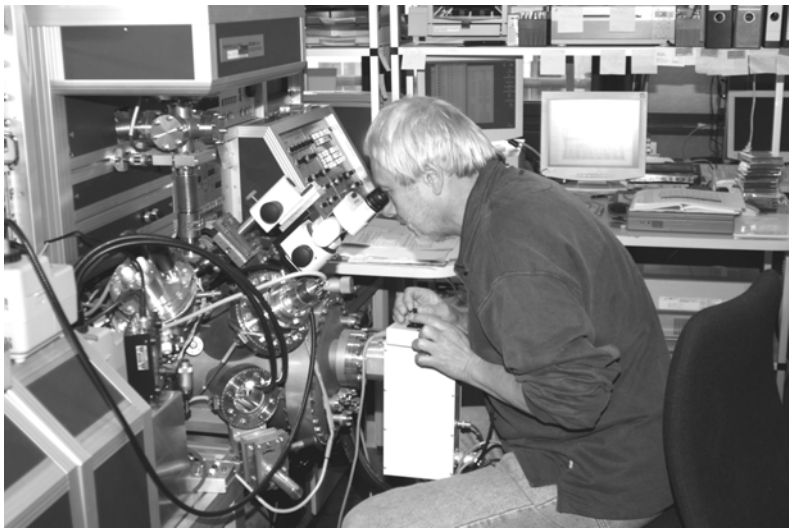

3.7 Gruppe Bauelementanalyse / *Group Device Analysis*

Gruppenleiter/Group Leader: UWE RAU
Mitarbeiter/Collaborators: Gregor Kron, Julian Mattheis, Viet Nguyen, Kurt Taretto-Zeyen, Mircea Turcu, Kristin Weinert

Die Gruppe *Bauelementanalyse* befaßt sich mit der elektrischen und optischen Charakterisierung sowie der numerischen Simulation von Solarzellen basierend auf CdS/Cu(In,Ga)Se_2 und a-Si:H/c-Si Heterostrukturen sowie von Farbstoff-Solarzellen auf der Basis von nano-porösem TiO_2. Ziel unserer Aktivitäten ist ein grundlegendes Verständnis der Funktionsweise dieser Baulemente, des Einflusses der Präparationsbedingungen und des Designs des Baulements auf seine Leistungsfähigkeit. Wir benutzen elektrische Analysemethoden wie Strom-Spannungsmessungen, Admittanzspektroskopie und Transienten-Spektroskopie tiefer Störstellen (DLTS). Messungen der internen Quantenausbeute und Photolumineszenz dienen zur Untersuchung der elektro-optischen Eigenschaften der Materialien. Die experimentellen Resultate werden mit quantitativen, numerischen wie analytischen, Modellen verglichen, um ein kohärentes Verständnis der Bauelemente zu erhalten.

The *device analysis* group is concerned with the electrical and optical characterization and with the numerical simulation of large-area electronic devices such as solar cells based CdS/Cu(In,Ga)Se_2 and a-Si:H/c-Si heterojunctions as well as dye-sensitized solar cells based on nano-porous TiO_2. We focus on a fundamental understanding of the working principle of these devices, the influence of preparation conditions and device design on the performance and, finally, on the improvement and optimization. Electrical analysis is performed with the help of current-voltage measurements, admittance spectroscopy, Deep Level Transient Spectroscopy (DLTS), and similar methods. Electro-optical analysis comprises measurements of internal quantum efficiency, optical transmittance and reflectance, photoluminescence, etc. The quantitative and coherent interpretation of these experimental results requires detailed modeling and simulation.

Gruppe Bauelementanalyse / *Group Device Analysis :*
Von links *(from left)* : Mircea Turcu, Julian Mattheis, Viet Nguyen, Gregor Kron, Uwe Rau, Kristin Weinert, Kurt Taretto.

Kontaktierung von Solarzellen zur anschließenden elektrischen Charakterisierung.

Preparation of solar cells for electrical characterisation.

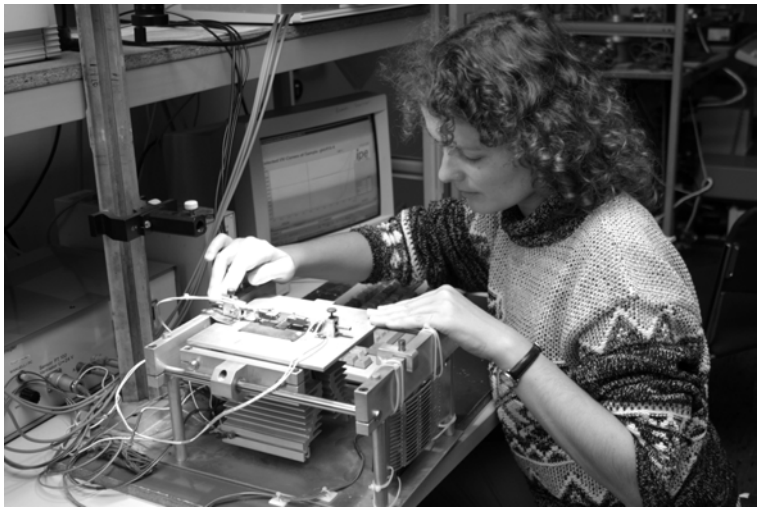

4 Wissenschaftliche Beiträge / *Scientific Contributions*

4.1 Effects of 3-MeV Electron Irradiation on Cu(In,Ga)Se$_2$ Solar Cells

Author: K. WEINERT
In collaboration with: U. Rau, A. Jasenek, H. W. Schock, J. H. Werner, B. Schattat [1], W. Bolse[1]

Solar cells based on Cu(In,Ga)Se_2 absorber layers have the highest conversion efficiency of all photovoltaic thin-film technologies. In addition to the possibility to prepare this material on low-weight and flexible substrates, the extraordinarily high radiation resistance against proton and electron irradiation makes this type of solar cells attractive for space applications. However, the radiation response of these devices has to be carefully analyzed in order to predict their performance under space conditions.

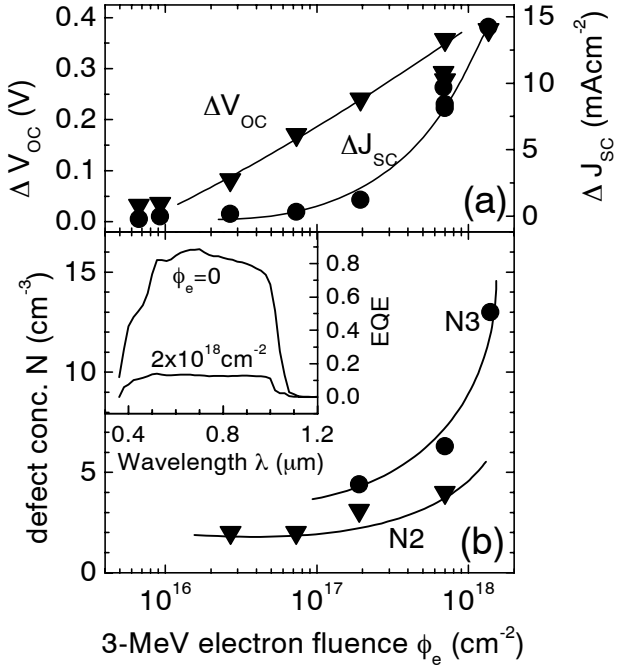

Figure 1: (a) Open circuit voltage - and short circuit current losses ΔV_{OC} and Δj_{SC} after 3-MeV electron irradiation with different fluences ϕ_e of 3-MeV electrons. (b) Increase of the defect concentration N of the defects N2 and N3 with increasing electron fluence ϕ_e. Inset: External quantum efficiency EQE before and after the 3-MeV electron irradiation with $\phi_e = 2\times10^{18}$ cm^{-2}.

In the following, we focus on irradiation experiments with *3-MeV electrons* [1]. Figure 1 a shows that the degradation of the conversion efficiency η between a fluence ϕ_e of 2×10^{16} cm^{-2} and 2×10^{17} cm^{-2} is predominantly caused by a reduction of V_{OC}. Additionally, we observe a

[1] *Institut für Strahlenphysik, Universität Stuttgart*

decrease of the short circuit current density J_{SC} at fluences ϕ_e higher than 2×10^{17} cm^{-2}. External Quantum Efficiency (EQE) measurements (inset of Fig. 1) show that the loss of ΔJ_{SC} of J_{SC} to be uniform over the entire spectral range of light absorption in the solar cell. This decrease of J_{SC} is linked to the occurrence of a peak N3 at an activation energy of 500 meV in the admittance defect spectra of the irradiated solar cells [1]. Note that a similar defect was not observed during earlier irradiation experiments [2] using 1-MeV electrons. Since the concentration of the defect N3 increases at fluences above $\phi_e \approx 2\times10^{17}$ cm^{-2} , i.e., at the same threshold as the decline of J_{SC}, we assume that the generation of N3 is the origin of the J_{SC} degradation.

The thermal annealing experiments of Fig. 2 also indicate that the loss of J_{SC} and that of V_{OC} have different physical origins because their respective annealing temperatures of about 350 K and 420 K are significantly different.

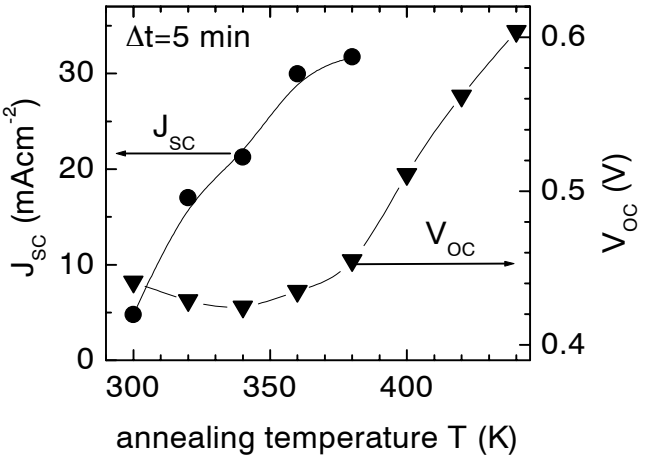

Figure 2: Recovery of short circuit current J_{SC} and open circuit voltage V_{OC} after isochronal annealing steps of fixed time Δt at temperatures T, that are successively increased by ΔT = 20 K. The recovery of J_{SC} occurs at significantly lower temperatures than that of V_{OC}, indicating that the two loss processes originate from two different physical mechanisms.

References:

[1] K. WEINERT, A. JASENEK, AND U. RAU, Thin Solid Films (in print).

[2] A. JASENEK AND U. RAU, J. Appl. Phys. **90**, 650 (2001).

4.2 Illumination-Enhanced Recovery of Cu(In,Ga)Se$_2$ Solar Cells after High-Energy Electron Irradiation

Author: A. JASENEK
In collaboration with: K. Weinert, H. W. Schock, U. Rau, J. H. Werner, B. Schattat [1], W. Bolse[1]

Thin-film heterojunction solar cells with polycrystalline Cu(In,Ga)Se$_2$ (CIGS) absorber layers show an extraordinary radiation hardness [1] that makes them attractive for extraterrestrial applications. The performance of solar cells in space is usually extrapolated from terrestrial irradiation experiments with electrons and protons at various energies. These experiments usually neglect the healing of irradiation-induced defects by elevated temperatures and by illumination. Since both, temperatures above 300 K as well as the presence of light, are part of the operation conditions, a proper prediction of the performance of solar cell in space environment has to take into account both types of annealing effects. Recent thermal annealing experiments unveiled thermally activated healing of *electron*-irradiated CIGS solar cells with an activation energy $E_a \approx 1.05$ eV and an (extrapolated) time constant $\tau = 2\times10^6$ s (i. e. about 1 month) at 330 K [2].

The present work addresses illumination-induced annealing of CIGS solar cells after irradiation with 1-MeV *electrons* using fluences ϕ_e of approximately $\phi_e = 10^{18}$ cm^{-2}. Illumination with white light at an intensity of 100 mWcm^{-2} for 3 h at room temperature is sufficient to recover a stable value of more than 80 % of the initial efficiency of the devices [3]. However, we do *not* find an enduring, stable recovery resulting from minority carrier injection by forward biasing the devices *in the dark* even when using current densities as high as 200 mAcm^{-2}.

Figure 1 illustrates the absence of enduring (dark-) injection annealing as well as the illumination enhancement of recovery of CIGS solar cells. In the dark experiment, the forward current density applied to solar cell A is 80 mAcm^{-2} for 24 h and, subsequently, 200 mAcm^{-2} for another 24 h. Note that the flux of photons absorbed in a CIGS solar cell under 1 sun illumination corresponds approximately to a current density of 40 mAcm^{-2}. Thus, the current densities under the above bias conditions are two and five times larger than the recombination current density under 1 sun illumination. During our dark injection experiment, the irradiation

[1] *Institut für Strahlenphysik, Universität Stuttgart*

induced loss ΔV_{OC} (squares) of the open circuit voltage decreases from approximately 160 mV to about 110 mV after the first day and further to 100 mV after the second day. For the illumination experiment shown in Fig. 1, the solar cell is exposed to white light with an intensity of 100 mWcm^{-2} and kept under open circuit conditions. Not only is the time constant for the re-increase of V_{OC} of cell B much shorter than that of cell A, but also, the increase of V_{OC} by (dark-) injection is not enduring like in the case of illumination-annealing. Re-inspection of the solar cell A after one and after 28 days unveils that V_{OC} relaxes almost to the value prior to the injection treatment, whereas V_{OC} of cell B only relaxes by about 10 mV during 50 days, i.e., the illumination-induced recovery by more than 70 mV is stable. Thus, we ascribe the intermediate increase of V_{OC} by electron injection in the dark to the metastable and reversible V_{OC} enhancement commonly observed in CIGS solar cells upon minority carrier injection [4]. In contrast, an *enduring annealing* of radiation-induced defects occurs after direct exposure of the solar cell to light.

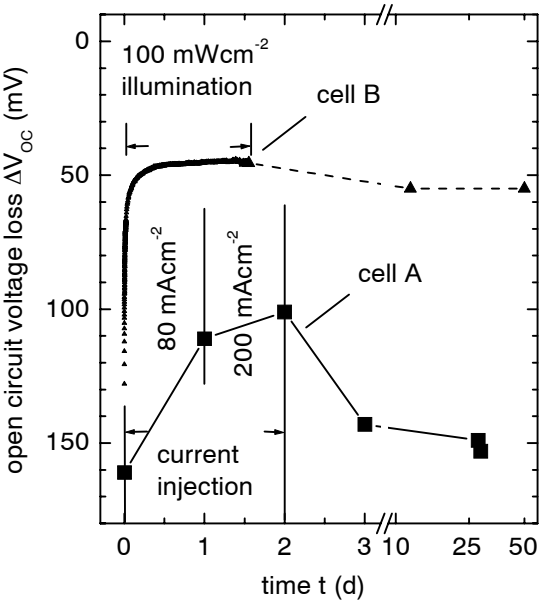

Figure 1: Open circuit voltage loss ΔV_{OC} of a CIGS solar cell after electron irradiation. During current injection (cell A) with current densities of 80 mAcm^{-2} and 200 mAcm^{-2}, ΔV_{OC} decreases from 160 mV to about 110 mV and, further, to 100 mV. This recovery, however, is metastable and drops back close to the value prior to current injection. The upper curve for cell B illustrates the recovery of V_{OC} during 1.5 days of illumination under open circuit conditions. The recovery of ΔV_{OC} proves to be enduring for at least 50 days.

References:

[1] A. JASENEK AND U. RAU, J. Appl. Phys. **90**, 650 (2001).

[2] A. JASENEK, H. W. SCHOCK, J. H. WERNER, AND U. RAU, Appl. Phys. Lett **79**, 2922 (2001).

[3] A. JASENEK, U. RAU, K. WEINERT, H. W. SCHOCK, AND J. H. WERNER, in *Proc. 29th IEEE Photov. Spec. Conf. (2002, in print)*.

[4] U. RAU, M. SCHMITT, J. PARISI, W. RIEDL, AND F. KARG, Appl. Phys. Lett. **73**, 223 (1998).

4.3 Influence of Cu-Stoichiometry on the Recombination Mechanism in Cu(In,Ga)(S,Se)$_2$ Solar Cells

Author: M. TURCU
In collaboration with: O. Pakma [1], U. Rau

Cu-chalcopyrites such as Cu(In,Ga)Se_2 provide the absorber material for the to date most efficient thin-film solar cells. Using the complete alloy system Cu($In_{1-x}Ga_x$)($Se_{1-y}S_y$)$_2$ instead of the standard material Cu($In_{1-x}Ga_x$)Se_2 with a moderate Ga-content of $x \approx 0.2$ is interesting when aiming at high open circuit voltage solar cells. The band gap energy E_g of $CuInSe_2$ increases upon alloying with Ga and/or S. However, solar cells based on those wide-gap Cu-chalcopyrites generally deliver a significantly lower device performance compared to the lower-gap devices. The main drawback of those solar cells is the fact that the open circuit voltage V_{OC} does not increase at the same rate as E_g. Thus, it appears that the recombination mechanism changes either qualitatively or quantitatively upon alloying $CuInSe_2$ with Ga and/or S. It is, however, unclear whether this trend results from lower-grade bulk properties of the wide-gap absorber [1] or from the less favorable band offset between the CdS window layer and the wide-gap chalcopyrite [2].

This study uses temperature-dependent current-voltage measurements to determine the dominant recombination path in thin-film heterojunction solar cells based on a variety of Cu(In,Ga)(Se,S)$_2$ alloys [3,4]. We use thin films with a final Cu-poor stoichiometry as well as films with a Cu-rich composition (prior to KCN etching) as starting material for device fabrication. We determine the activation energy E_a of the recombination process in each Cu(In,Ga)(Se,S)$_2$ solar cell by measuring the temperature T dependence of the open circuit voltage V_{OC} tand extrpolating the results to $T = 0$ K, as well as using corrected Arrhenius plots of the saturation current density. As shown in Fig. 1, the activation energy E_a of recombination follows the band gap energy of the respective Cu(In,Ga)(Se,S)$_2$ alloy as long as the films are grown with a Cu-poor final composition. Thus, electronic loss in these devices is dominated by recombination in the bulk of the absorber material. In contrast, all devices based on absorber alloys with a Cu-rich composition prior to heterojunction formation are dominated by recombination at the heterointerface, with activation energies smaller than the band gap energy of the absorber material. These activation energies are

[1] *Faculty of Arts and Science, University of Mugla, Turkey*

independent from the S/Se-ratio but increase with increasing Ga/In ratio. This beneficial effect of Ga is compatible with earlier findings that the Fermi-level pinning at the CdS/Cu(In,Ga)(Se,S)$_2$ interface is closer to conduction band when alloying CuInSe$_2$ with Ga as compared to alloying with S [5].

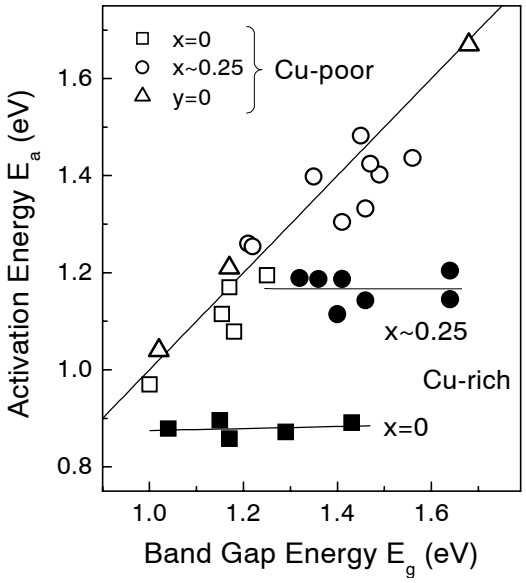

Figure 1: *The activation energy* E_a *of the recombination process as a function of the band gap energy* E_g *of the absorber material for ZnO/CdS/Cu(In*$_{1-x}$*Ga*$_x$*)(Se*$_{1-y}$*S*$_y$*)*$_2$ *heterojunctions. The activation energy for the Cu-poor devices follows the band gap energy of the absorber material. In case of Cu-rich devices, the activation energy is independent on the band gap energy* E_g *as long as the variation of* E_g *is achieved by varying S/(S+Se) ratio* y *at a constant Ga/(Ga+In) ratio* x.

References:

[1] G. HANNA, A. JASENEK, U. RAU, AND H. W. SCHOCK, Phys. Stat. Sol. (a) **179**, R7 (2000).

[2] R. HERBERHOLZ, V. NADENAU, U. RÜHLE, C. KÖBLE, H. W. SCHOCK, AND B. DIMMLER, Solar Energy Mat. Solar Cells **49**, 227 (1997).

[3] M. TURCU, O. PAKMA, AND U. RAU, Appl. Phys. Lett. **80**, 2598 (2002).

[4] M. TURCU AND U. RAU, Thin Solid Films. (2002, in print).

[5] M. TURCU, I. M. KÖTSCHAU, AND U. RAU, J. Appl. Phys. **91**, 1391 (2002).

4.4 Diffusion Limitations in Nanoporous TiO_2 Networks

Author: G. KRON
In collaboration with: M. Duerr[1], T. Miteva[1], G. Nelles[1], A. Yasuda[1], U. Rau, J. H. Werner

Dye sensitized solar cells (DSSC) use a network of nanoporous TiO_2 covered by a monolayer of dye molecules [1] to enhance the effective surface area for light absorption. According to the reaction $3I^- \leftrightarrow I_3^- + 2e^-$, the I^- in the electrolyte reduces the dye molecule after photoinjection and the oxidized species I_3^- diffuses to the platinum (Pt) back electrode. The concentration of I_3^- ions in a standard DSSC is one order of magnitude smaller than that of I^- [2]. Therefore, the diffusion of the I_3^- ions through the TiO_2 network plays an important role and could be a limiting factor for the efficiency of the DSSC.

For determination of the limiting current density j_{lim}, we use a DSSC-like device structure where a non-dyed nanoporous TiO_2 layer is sintered directly onto a Pt electrode instead of using a SnO_2:F electrode [3]. The electronic transport in such a device is dominated by the catalytic reaction at the Pt/electrolyte interface. Diffusion of I_3^- through the network is directly connected in series to the catalytic reaction and, as soon as the limiting diffusion current density is achieved, the current voltage characteristic enters a saturation regime. After further increase of the voltage, electronic transport is taken over by electron injection into the TiO_2 and reduction of I_3^- at the TiO_2/electrolyte interface, and the current density levels off from the diffusion plateau.

We produce devices of the type described above with different TiO_2 layer thicknesses d and we use different I_3^--concentrations c_T in the electrolyte. Figure 1 (a) shows j_{lim} plotted versus the I_2-concentration c_{I2}, that equals the I_3^-–concentration c_T. Figure 1 (b) depicts the inverse limiting current density $1/j_{lim}$ versus d. The limiting current density through a nanoporous layer of thickness d is given by [4]

$$j_{lim} = 2qc_T^d D_T^{eff}/d\,, \qquad (1)$$

with the effective diffusion constant D_T^{eff} in the nanoporous medium and the Triiodide concentration c_T^d at the end of the layer. In Fig. 1 (a), we

[1] *Sony International (Europe) GmbH, MSL, Stuttgart, Germany*

observe a linear increase of j_{lim} with increasing c_{I2}. Extrapolation of the data to $c_{I2} = 0$ yields $j_{lim} > 0$. Thus, the measured values contain an offset by a parallel current path that is due to the Li^+/I^- system only. In order to investigate I_3^-–diffusion, we must correct all experimental data with the help of a reference measurement using a device with the same d but without adding I_2. Figure 1 (b) compares uncorrected and corrected data. The axis intercept of the corrected data (nanoporous layer thickness d =0) in Fig. 1 (b) depends on the I_3^--diffusion in the bulk of the electrolyte only, whereas the slope of the line reflects diffusion through the network and finally yields D_T^{eff}. From our experimental data we find diffusion constants $D_T = 1.24\times10^{-5}$ cm^2s^{-1} for the bulk and and $D_T^{eff} = 4.45\times10^{-6}$ cm^2s^{-1} for the network. Thus, the effective diffusion constant D_T^{eff} is about one third of the bulk value because of transport restrictions in the nanoporous network.

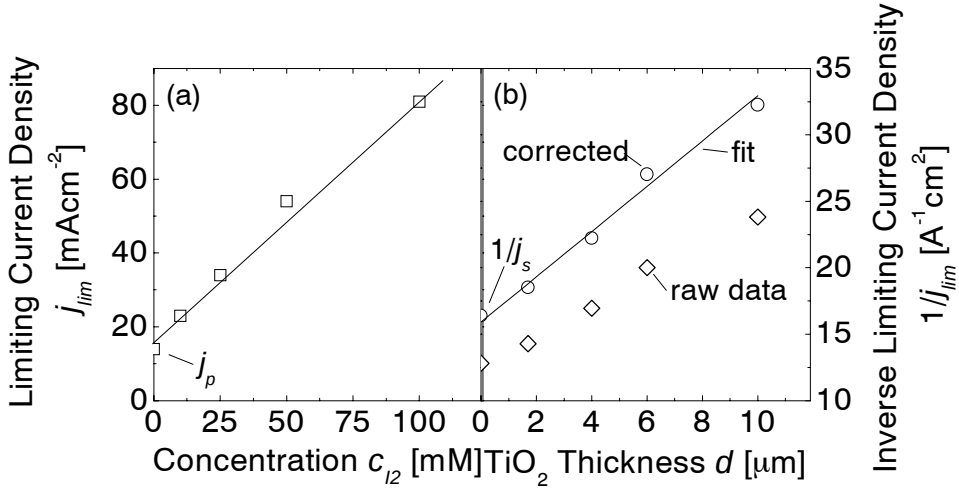

Figure 1: (a) Limiting current density j_{lim} of a series of devices with TiO_2 layer thickness d = 6 μm plotted vs. the iodine concentration c_{I2} in the electrolyte. The y-axis intercept j_p results from a parallel diffusion current. (b) Inverse limiting current densities $1/j_{lim}$ plotted vs. different TiO_2 layer thicknesses d with the standard I_2-concentration c_{I2} = 50 mM. Diamonds correspond to the data that are not corrected for the parallel current density j_p, circles are values corrected for j_p. The axis intercept of the corrected data depends on the I_3^--diffusion constant D_T in the bulk of the electrolyte, whereas the slope of the line finally yields D_T^{eff} in the network

References:

[1] B. O'REGAN AND M. GRAETZEL, Nature **353**, 737 (1991).

[2] N. PAPAGEORGIOU, Y. ATHANASSOV, M. ARMAND, P. BONHOTE, H. PETTERSSON, A. AZAM, AND M. GRAETZEL, J. Electrochem. Soc. **143**, 3099 (1996).

[3] N. PAPAGEORGIOU, C. BARBE, and M. GRAETZEL, J. Phys. Chem. B **102**, 4156 (1998).

[4] A. HAUCH AND A. GEORG, J. Electrochim. Acta **46**, 3457 (2001).

4.5 Simple Method to Extract the Diffusion Length from Output Parameters of Solar Cells - Application to Polycrystalline Silicon

Author: K. TARETTO
In collaboration with: U. Rau, J. H. Werner.

The efficiency of solar cells depends strongly on the effective diffusion length L_{eff} of minority carriers. Usually, evaluation of Internal Quantum Efficiency (IQE) measurements give L_{eff}, but its determination is based on an exact knowledge of the absorption and dispersion of light in the cell. Unfortunately, the absorption data of thin-film materials is often not available.

In this work we obtain an equation that permits a simple estimate of L_{eff} without knowing the absorption constant of the material [1]. We calculate L_{eff} directly from the open circuit voltage V_{OC}, the short circuit current density J_{SC}, and the doping level N_A in the base of the solar cell. Our approach is based on the current/voltage characteristics of a *pn* cell where the open circuit voltage is allowed to be controlled by recombination in the neutral regions as well as in the space charge regions. Figure 1 shows the relationship between L_{eff}, V_{OC}, J_{SC}, and N_A established by our model. To prove the validity of our approach, we compare a large data set of L_{eff} measured by IQE with the predictions of our model. We show that throughout *three orders of magnitude* of L_{eff}, our method allows to determine L_{eff} within an accuracy of better than 35 %.

In the second part of this work, we utilize our method to determine L_{eff} to investigate the role of grain boundary recombination in polycrystalline silicon solar cells by means of the dependence of L_{eff} on grain size g (see Ref. [1]). Our analysis considers literature data of solar cells with grain sizes in the range $10^{-2} < g < 10^{4}$ µm. We model the resulting $L_{eff}(g)$ dependence as a function of grain size g and the recombination velocity S_{GB} at the grain boundaries. This modeling reveals that at $g > 1$ µm, most cells show values of S_{GB} between 10^5 and 10^7 cm/s, while cells with $g < 1$ µm are only understood with S_{GB} between 10^1 and 10^3 cm/s. An explanation for such low grain boundary recombination velocities is given in Ref. [2], where it was argued that the low S_{GB} comes from *structural* differences between the cells with $g < 1$ µm and cells showing $g > 1$ µm. This suggestion was based on the fact that *all efficient* cells with $g < 1$µm were reported to have a {220} surface texture. Thus, the measured {220}-texture implies a (110)-oriented surface for most of the grains. A large number of the columnar

grains must therefore be separated by [110] tilt grain boundaries. Symmetrical grain boundaries of this type are electrically inactive because they contain no broken bonds.

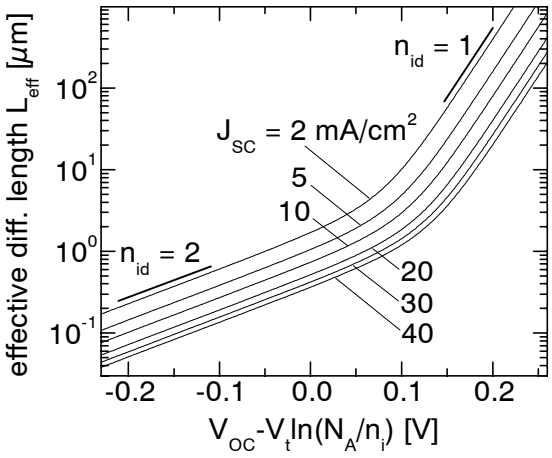

Figure 1: Effective diffusion length L_{eff} obtained by the model, as a function of open circuit voltage V_{OC}, doping level N_A in the base of the solar cell, and short circuit current density J_{SC}. At low L_{eff}, the curves are described by recombination in the space charge region (ideality n_{id} = 2). At high L_{eff}, the recombination in the base (n_{id} = 1) limits V_{OC}.

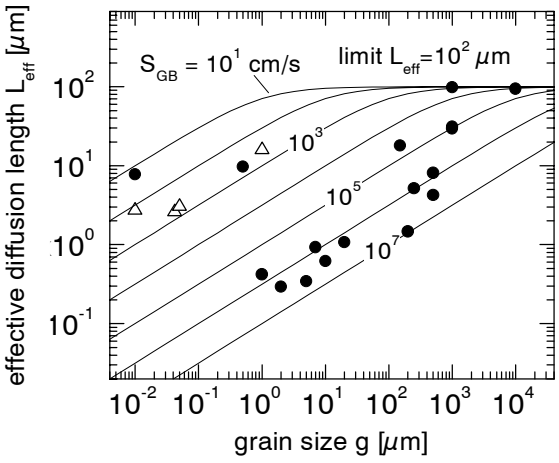

Figure 2: Data points give the diffusion length L_{eff} extracted from literature data using Figure 1. Circles correspond to np cells and triangles to pin cells. The solid lines model L_{eff} considering a recombination velocity S_{GB} at the grain boundaries.

References:

[1] K. TARETTO, U. RAU, AND J. H. WERNER, in *Polycrystalline Semiconductors VII*, ed. by T. FUYUKI, T. SAMESHIMA, H. P. STRUNK, AND J. H. WERNER, Solid State Phenomena (Scitec, Zurich, 2003), in print.

[2] J. H. WERNER, in *Techn. Dig. 13th Sunshine Workshop on Thin Film Solar Cells*, ed. by M. KONAGAI (NEDO, Tokyo, Japan, 2000), p. 41.

4.6 Interface Recombination at a-Si:H/c-Si Heterointerfaces

Author: V. X. NGUYEN
In collaboration with: M. Rakhlin, K. Brenner, U. Rau, J. Mattheis, J. H. Werner

Heterojunction solar cells consisting of an amorphous hydrogenated silicon (a-Si:H) film on top of a crystalline silicon (c-Si) absorber are a technological alternative to c-Si solar cells with diffused pn-junctions. Processing of a-Si:H/c-Si solar cells is comparatively simple and the heterojunction is formed by depositing a highly doped a-Si:H layer onto a crystalline silicon wafer at temperatures below 200°C. The high potential of this technology was demonstrated by a record cell with the so-called HIT structure (Heterojunction with Intrinsic Thin layer between a-Si:H emitter and c-Si base) having an efficiency of η=20.7 % and an open circuit voltage of V_{oc} =719 mV [1]. This cell consisted of an n-type c-Si absorber with a p-type a-Si:H heterojunction partner and an n-type a-Si:H back contact. Efficiencies of the inverse doping sequence, i.e., n-type a-Si:H emitter with p-type c-Si base, are limited by a relatively lower V_{oc}, the highest value reported up to now being 655 mV [2].

The present work uses quasi-steady-state photoconductance (QSSPC) lifetime measurements [3] to investigate the recombination velocity at the a-Si:H/c-Si heterointerface. Hereto we deposit (i)a-Si:H followed by an n- or p-type doped layer symmetrically on both surfaces of c-Si wafers. We obtain four different structures : pi/p/ip and ni/p/in on p-type wafers (0.35 Ωcm, 375 μm thickness) and pi/n/ip and ni/n/in on n-type wafers (1 Ωcm, 250 μm thickness). Similarly, as reported in Ref. [4], we find the interface recombination velocity of all structures to drastically decrease after annealing the samples for 10 min at 200-250 ^{0}C. Figure 1 shows that the interface recombination velocities of n-type wafers (pi/n/ip as well as ni/n/in-structures) are lower than those on p-type wafers. Especially, a value of 250 cm/s found for the ni/p/in-structure appears still unsatisfactory as the (n)a-Si/(p)c-Si heterointerface is the phototovoltaically active interface in the finished solar cell.

The higher V_{oc} potential of the (p)a-Si/(n)c-Si heterostructure can be directly judged from measuring the implicit V_{oc} vs. illumination intensity curves [3] obtained from QSSPC measurements performed at pi/n/in and ni/p/ip structures. The measurements in Fig.2 show that a heterojunction solar cell using an n-type absorber has a V_{oc} potential of above 700 mV (at 1 sun), whereas the (n)a-Si/(p)c-Si structure has only a potential of 675 mV. The major reason for this lower potential lies in the built-in

voltage of the (n)a-Si/(p)c-Si structure that is lower than that of the (n)a-Si/(p)c-Si structure [2].

We further perform optimization of the thickness of the two a-Si:H emitter layers with the help of QSSPC and by investigating completed heterojunction solar cells. The optimum emitter thickness for (n)/(i)a-Si/(p)c-Si heterojunctions is about 8 nm (n) and 6 nm (i) (both layers deposited in 45 seconds). With these optimum thicknesses, our best solar cell now has an independently confirmed efficiency of 15.44 % (short circuit current densitiy J_{SC} = 29.44 mA/cm^2, V_{OC} = 658.5 mV, and fill factor *FF* = 79.5%).

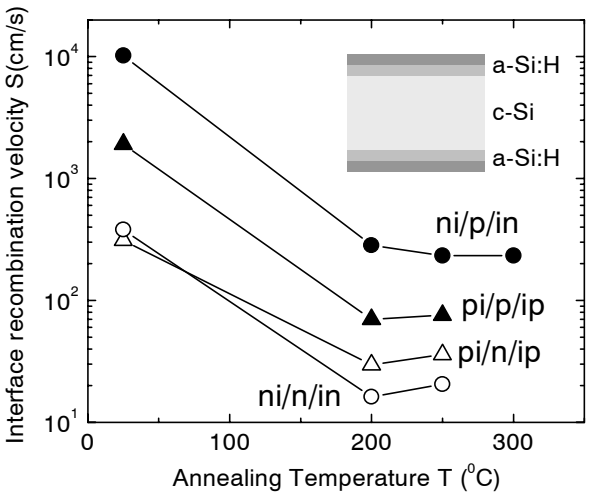

Figure 1: Effect of annealing for 10 min at various temperatures on the a-Si:H/c-Si interface recombination velocity. Data are obtained from quasi-steady-state photoconductance (QSSPC) measurements on p-type and n-type c-Si wafers with symmetrically deposited (p)/(i) and (n)/(i) a-Si:H double layers. Inset shows the investigated structure with two a-Si:H double layers on both sides of the c-Si wafer.

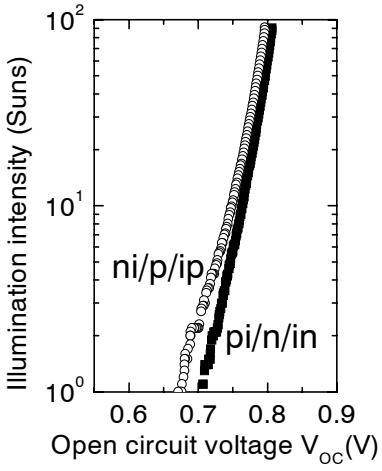

Figure 2: Implicit open circuit voltage from QSSPC measurements for HIT structures on p-type (ni/p/ip) and on n-type wafers (pi/n/in).

References:

[1] H. SATAKA, T. NAKAI, T. BABA, M. TAGUCHI, S. TSUGE, K. UCHIHASI, AND S. KYIAMA, in *Proceedings 28th IEEE Photovoltaic Specialists Conference* (IEEE, New York, 2000) p. 7.

[2] N. JENSEN, R. M. HAUSNER, R. B. BERGMANN, J. H. WERNER, AND U. RAU, Prog. Photovolt. Res. Appl. **10**, 1 (2002).

[3] R. A. SINTON AND A. CUEVAS, Appl. Phys. Lett. **69**, 2510 (1996).

[4] S. DAUER, J. SCHMIDT, AND R. HEZEL, in *Proceedings 29th IEEE Photovoltaic Specialists Conference* (IEEE, New York, 2002) in print.

4. 7 Alternative Back Contact Materials for Cu(In,Ga)Se_2 Thin-Film Solar Cells

Author: K. ORGASSA
In collaboration with: H. W. Schock, J. H. Werner

The requirements for a good back contact material for Cu(In,Ga)Se_2 (CIGS) solar cells are manifold. A certain inertness of the contact material is the prerequisite for reproducible CIGS absorber growth in the highly corrosive process atmosphere during the CIGS deposition. The contact layer must function as barrier for diffusion of impurities from the substrate into the absorber. For good electronic device properties, the formation of an ohmic contact for the majority carriers (holes) from the p-type CIGS and a low recombination rate for the minority carriers (electrons) at the CIGS / back contact interface is essential. Finally, a high optical reflectance is necessary to minimize optical losses. Molybdenum, the "historical" back contact material for CIGS solar cells, complies well with most requirements. Mo is inert during the deposition, allows for the growth of large grains, and forms an ohmic contact via an intermediate $MoSe_2$ layer [1]. However, there is hardly any literature on CIGS solar cells on alternative back contact materials.

In this study we investigate Cu(In,Ga)Se_2 thin-film solar cells on a variety of different back contact metals (W, Mo, Cr, Ta, Nb, V, Ti, Mn) on glass substrates. During the Cu(In,Ga)Se_2-deposition, the metal contacts W, Mo, Ta, and Nb are almost inert, whereas Cr, V, Ti, and Mn tend to react with Se. The reaction of Se with the latter metals advances during the entire CIGS deposition. In case of Ti and Mn, the metal films are completely consumed by the chemical reaction, even for short CIGS deposition times of about t = 12 min. As a consequence, we were unable to fabricate solar cells on these substrates.

We fabricate absorber layers by co-evaporation from elemental sources: A first set with homogeneous CIGS composition, and a second set, in which we integrate a Ga-rich growth step at the begin of the CIGS deposition in order to realize a graded bandgap [2] at the back contact. This "back surface grading" provides a barrier for minority carriers (electrons) diffusing towards the back contact. Figure 1 displays the open circuit voltage V_{oc} of Cu(In,Ga)Se_2 solar cells on W, Mo, Ta, and Nb. For solar cells without graded gap (squares), we observe a successive decrease of the open circuit voltage for different back contacts in the order W, Mo, Ta, Nb. If we introduce a Ga-gradient at the

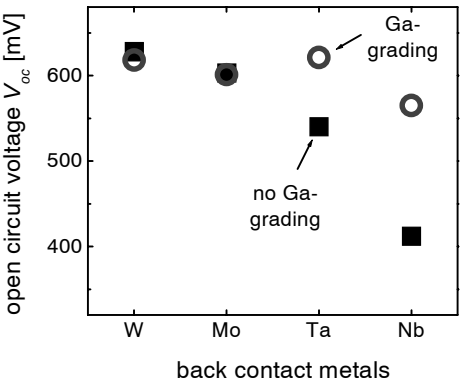

Figure 1: Open circuit voltage V_{oc} of solar cells with W, Mo, Nb, and Ta back contacts. Open circles present cells with Ga-grading at the backside, squares cells without. In case of Ta and Nb, the Ga-grading passivates the absorber / back contact interface.

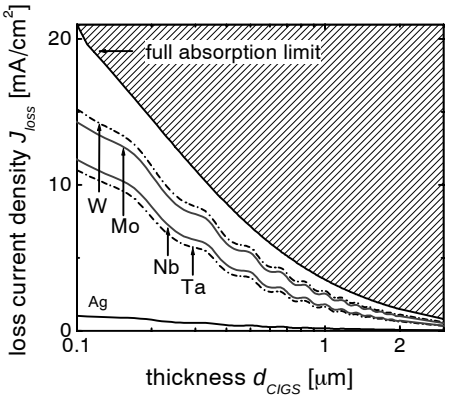

Figure 2: Simulation of the optical absorption of different back contact metals in CIGS solar cells as a function of thickness d_{CIGS}. J_{loss} is the current density that is lost in the back contact by optical absorption.

CIGS back side (open circles), the open circuit voltage V_{oc} of devices with W or Mo remains unchanged, whereas V_{oc} of devices with Ta or Nb contacts almost increases to that of W or Mo. This result indicates, that the interfaces CIGS / Ta or CIGS / Nb are passivated by the graded bandgap at the back side, whereas the contacts W and Mo provide a sufficient self-passivation. The best total-area device efficiencies obtained are 14.2 % on W, 13.8 % on Mo, 13.3 % on Ta, 10 % on Nb, 5.9 % on Cr, and 3.4 % on V.

For decreasing absorber thickness the optical absorption losses at the back contact increases. Using an optical model of flat layers, we simulate the optical absorption at the back contact and calculate a corresponding current density loss J_{loss} for different back contact metals (Fig. 2). The simulation shows, that for thin CIGS absorber layers, absorption at back side causes significant losses. Since electrical losses at the back contact can be avoided by graded gap structures, the short-circuit current density J_{sc} in thin CIGS solar cells can be kept high by using light-trapping structures in combination with an alternative reflecting back contact metallization.

References:

[1] T. WADA, N. KOHARA, T. NEGAMI, AND M. NISHITANI, Jpn. J. Appl. Phys. **35**, L1253 (1996).

[2] T. DULLWEBER, O. LUNDBERG, J. MALMSTRÖM, M. BODEGARD, L. STOLT, U. RAU, H. W. SCHOCK, AND J. H. WERNER, Thin Solid Films **387**, 11 (2001).

4.8 Influence of Selenium Flux on Growth of Cu(In,Ga)Se2 Thin Films

Author: G. HANNA
In collaboration with: J. Mattheis, U. Rau, H. W. Schock

For large-scale production of solar cells based on $Cu(In,Ga)Se_2$ (CIGS) questions such as the minimal use of materials or the trade off between device quality and process time have gained more importance. In order to address the issue of Se consumption, we need a precise control of the elemental composition in the vapour flux, which is not easy to obtain due to the low sticking coefficient of selenium even onto cold substrates. With reliably calibrated fluxes, we identify the minimal selenium over-saturation necessary to obtain high-quality CIGS films.

Based upon the observation that co-evaporation of the metals enhances sticking of Se, we determine in a first step the selenium flux F_{Se} at a given rate control signal Q_{Se} for selenium. A simple growth model yields the relation between G_{Se}, which is the rate of selenium atoms finally sticking onto the substrate, and the metal and Se fluxes F_{Me}, F_{Se} according to

$$G_{Se} = \frac{\sigma_{Se}\tau F_{Se} + \sigma_{Me}\tau F_{Me}}{\sigma_{Se}\tau F_{Se} + \sigma_{Me}\tau F_{Me} + 1} F_{Se} \qquad (1)$$

The products $\sigma_{Se}\tau$ and $\sigma_{Me}\tau$ are two variables which account for the cross sections and time constant of condensation [1]. From measuring G_{Se} at different F_{Me} (but constant Q_{Se}) we obtain values for $\sigma_{Se}\tau$, $\sigma_{Me}\tau$, and finally F_{Se} by fitting Eq. (1) to the experimental data, as seen in Fig.1. Repeating the same procedure at different Q_{Se} leads to a new value of F_{Se}. By linear interpolation we get the desired calibration function $F_{Se}(Q_{Se})$. The values of $\sigma_{Se}\tau$ and $\sigma_{Me}\tau$ do not change when changing Q_{Se}. Calibrating the metal fluxes is more straightforward and described in [1].

With reliable calibration functions $F_{Se}(Q_{Se})$ and $F_{Me}(Q_{Me})$ we precisely adjust the selenium to metal flux ratio SMR = F_{Se}/F_{Me} during our CIGS co-evaporation processes. We systematically vary the SMR between 0.5 and 13.5 at short (25 min) and long (75 min) deposition times for 2 µm thick CIGS layers. The efficiencies of solar cells made from these absorbers in Figure 2 display a clear dependence of the cell efficiencies on both, the SMR and the deposition rate. Starting at low SMR, we get working devices (η > 0%) at SMR = 1.5 for fast and at SMR = 4.5 for slow processes. The best devices obtained from the fast processes

have an SMR = 4.5 while a higher SMR = 13.5 is needed to obtain comparable results from slow processes. These solar cells have an efficiency of η=14 %, a value that is expected from CIGS solar cells based on single-stage processes [2]. The poor performance of the cells at low SMR is explained by metal-rich (SMR $\leq$ 1.5) segregations or Na containing secondary phases (SMR = 4.5, slow process) [1].

Apparently, slow absorber deposition processes need much higher SMRs in order to result in solar cells with good performances than fast processes. Therefore, high rates allow to reduce the overall selenium consumption for the growth of efficient CIGS absorbers.

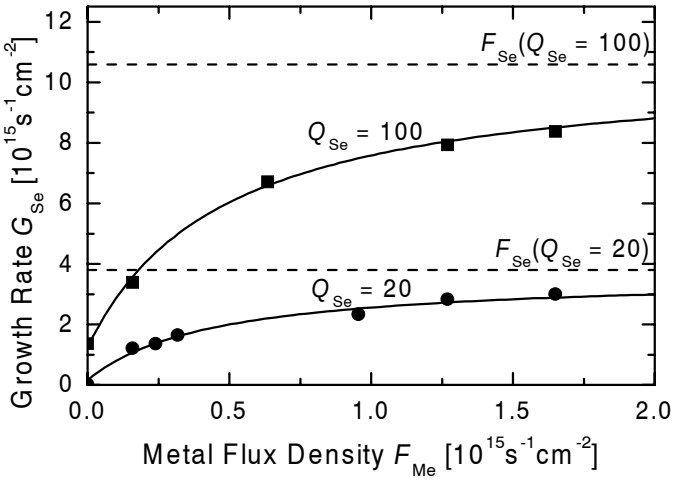

Figure 1: Growth rate of selenium G_{Se} plotted versus the co-evaporated metal flux F_{Me} at two measured selenium fluxes Q_{Se} = 20 and Q_{Se} = 100. The solid lines show the calculated values from Eq. (1) while the dashed lines indicate the values of the selenium flux F_{Se} corresponding to Q_{Se} = 20 and 100.

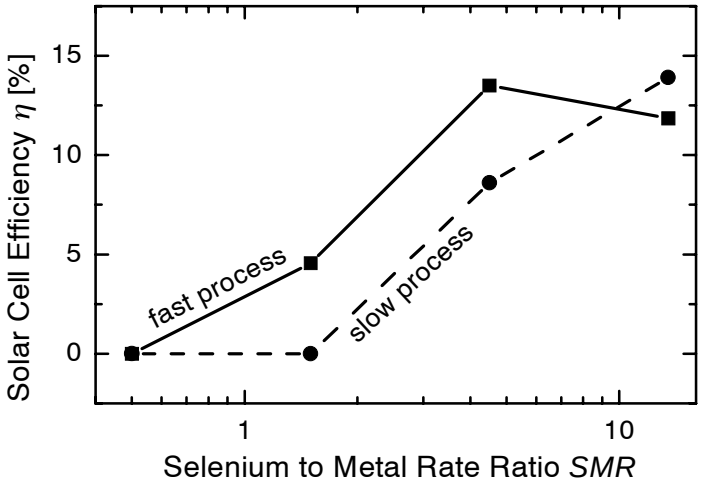

Figure 2: Solar cell efficiencies versus selenium to metal flux ratio SMR during growth of the solar cells absorber layer. The lines between the points are guides for the eye.

References:

[1] G. HANNA, J. MATTHEIS, V. LAPTEV, Y. YAMAMOTO, U. RAU, AND H. W. SCHOCK, Thin Solid Films (in print).

[2] G. HANNA, A. JASENEK, U. RAU, AND H. W. SCHOCK, Phys. Stat. Sol. (a) **179**, R7 (2000).

4.9 Electrical and Structural Investigations of Indium Sulfide Buffer Layers in Cu(In,Ga)Se_2 Solar Cells

Author: R. K. GEBHARDT
In collaboration with: V. Laptev, H. W. Schock

In Cu(In,Ga)Se_2 (CIGS) based solar cells the conventionally used CdS buffer layer in the heterojunction is deposited by a chemical bath procedure (CBD-CdS), which cannot be easily implemented in an in-line production process. Environmental reasons also necessitate research for alternative materials to CdS, e.g. indium sulfide.

In our experiments [1], the growth of indium sulfide buffer layers by co-evaporation immediately follows the absorber deposition without exposure to air in the same chamber (*in situ* preparation). Alternatively, we take CIGS absorber layers which have been exposed to air before deposition (*ex situ* preparation). We vary parameters for the growth of the buffer layer, i.e. the deposition temperature from 100°C to 320 °C and the In/S flux ratio. For the fabrication of solar cells, we deposit a ZnO:Al window layer either with or without an additional undoped i-ZnO layer by RF sputtering.

Structural investigations by gracing incidence X-ray diffraction in all cases only show phases with In_2S_3-stoichiometry. The In_2S_3-layers contain crystallites with tetragonal modifications, accompanied by rhombohedral and cubic structures. The high resolution scanning electron microscope picture of an In_2S_3 layer on a CIGS absorber in Figure 1 reveals a good coverage of the absorber layer at a thickness of the In_2S_3 layer of 30...60 nm and an abrupt In_2S_3/CIGS interface. The grains with a size of about 20 nm do not show a preferred orientation.

The performance of the solar cells improves with increasing deposition temperature for both kinds of preparation; the optimal value is found to be T_{dep} = 320 °C. Air-annealing of the cells improves performance. The optimal temperature is found to be T_{anneal} = 275...325 °C at an annealing time of about 30 min. The best cells reach 11% (*ex situ*) and 11.6 % efficiency (*in situ*). There is no significant difference in the performance of cells with or without additional i-ZnO layer. Short circuit currents J_{SC} of the cells with In_2S_3 buffer layers are comparable with those of the CBD-CdS reference cells, i.e. the higher performance of the reference cells results from a higher open circuit voltage and fill

factor. For the cells with In_2S_3-buffer layers V_{OC} = 609 mV was observed, CBD-CdS reference cells reach V_{OC} = 660 mV.

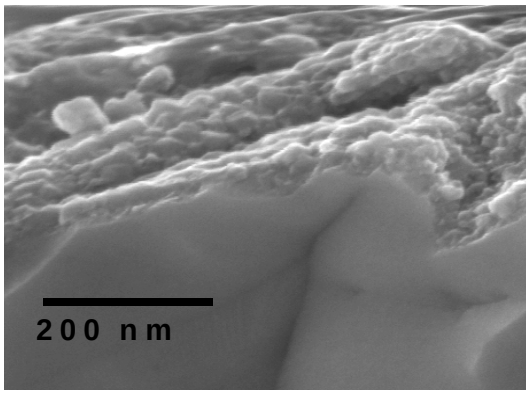

Figure 1: High-resolution scanning electron microscope picture of the abrupt interface between an In_2S_3 layer on top of the CIGS absorber film.

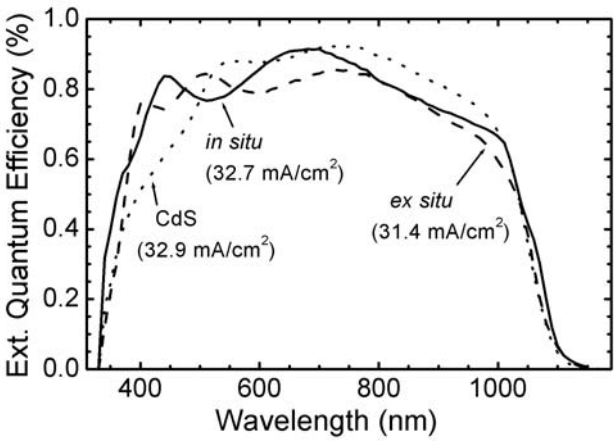

Figure 2: EQE of different cells (ex and in situ preparation) compared to the reference cell with CBD-CdS buffer layer.

Even though the bandgap of 2 eV of bulk In_2S_3 is smaller than that of CdS (2.4 eV), external quantum efficiency measurements (EQE) in Figure 2 show an improved blue response of the cells with In_2S_3 buffer layers as compared to reference cells with CdS buffer layers. In In_2S_3 grown by atomic layer deposition a high bandgap up to 3.3 eV is found [2]. The increase of the bandgap is explained by quantum size effects due to a small grain size. We find a similar increase of the bandgap of evaporated films. Reduced efficiencies of the cells with evaporated buffer layers result from lower quality of the interface between the absorber layers and the In_2S_3 buffer layers.

References:

[1] R. K. GEBHARDT, V. LAPTEV, AND H. W. SCHOCK, *Proc. Int. Conf. Ternary and Multinary Compounds*, (Paris 2002) to be published in J. Phys. Chem. Solids.

[2] E. B. YOUSFI, B. WEINBERGER, F. DONSANTI, P. COWACHE, AND D. LINCOT, Thin Solid Films **387**, 29 (2001).

4.10 Flexible Solar Cells on Thin-Film Transfer Silicon

Author: C. CRAFF CASTILLO
In collaboration with: C. Berge, W. Brendle, T. A. Wagner, M. B. Schubert, W. Appel[1], J. H. Werner

The detachment and transfer of thin, monocrystalline silicon films enables the fabrication of highly efficient, light-weight and flexible solar cells. Such bendable cells are particularly interesting for novel applications of photovoltaic energy supply, e.g. the integration of solar cells with garments and accessories, or even fabrics in general.

We have recently transferred thin-film silicon solar cells with a conversion efficiency of more than 14% onto flexible polyester foils. Similar cells transferred to rigid glass superstrates exhibit a world record efficiency of more than 16% [1]. Device simulation indicates an efficiency potential above 20% [2].

The key to fabricating flexible high-efficiency solar cells is the formation of porous silicon as a separation layer prior to device processing. Electrochemical etching and subsequent thermal re-structuring of the initially nano-porous layer generates a mechanically weak layer. Since the etching process requires fairly high doping levels of the starting wafer material ($4x10^{18}$- $2x10^{19}$ cm^{-3}), we form the photovoltaically active base region by epitaxy of 15 to 45 µm of p-type silicon on top of the separation layer [3]. As a pre-requisite for the growth of high-quality epitaxial silicon films, the pores in the surface of the re-structured seed layer completely close during the high temperature annealing at about 1100°C. The point defect and dislocation density in the electronically active epitaxial layer is not affected by the underlying separation layer.

All high-temperature processes for solar cell formation take place as long as the epitaxial film is still sticking to the silicon wafer. After processing, we detach the solar cell structure from the host wafer and transfer it to an arbitrary superstrate, e.g. a glass plate or a flexible polymer foil. Figure 1 shows flexible solar cells partially detached from the host wafer and transferred to a polyester foil. At thicknesses up to 50 µm, such thin-film cells are mechanically flexible, even though consisting of monocrystalline silicon. We access the front side contacts of the single cells through perforations in the plastic foil.

[1] Insitut für Mikroelektronik Stuttgart (ims-chips)

Figure 2 shows the current/voltage- (I/V-) characteristics of one of our first cells of 4 cm² size. With a thickness of 40 µm, these cells exhibit an efficiency of 14.6%, independently measured at the calibration lab of Fraunhofer Institute of Solar Energy Systems (FhG-ISE), Freiburg, Germany.

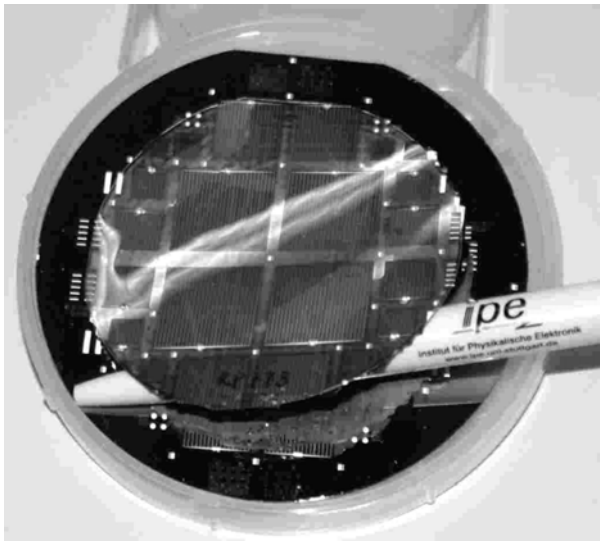

Figure 1: Flexible monocrystalline silicon solar cells, partially detached from the host wafer. A polyester foil sticks to the top surface of the cells, providing mechanical stability but still keeping the laminated compound flexible. We detach the thin-film Si cells from the wafer after the whole solar cell processing is completed (except for the back contact). Thereby we can apply standard wafer processing technology without any restrictions in temperature or handling.

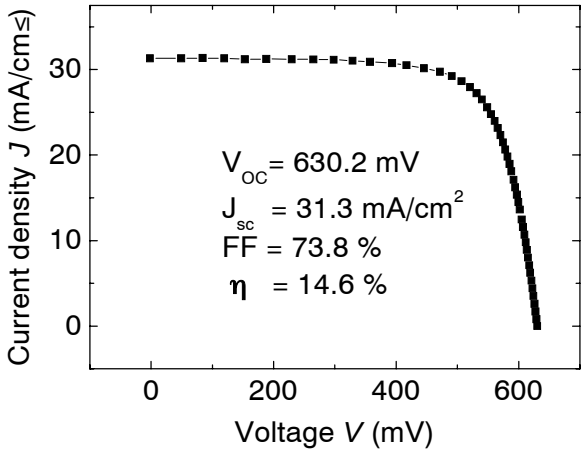

Figure 2: Current/voltage characteristics of a monocrystalline Si solar cell of an area of 4 cm² on polyester foil. With a thickness of 40 µm, this cell exhibits an efficiency of 14.6%, independently confirmed at the calibration lab of Fraunhofer ISE at Freiburg, Germany.

References:

[1] M. A. GREEN, Prog. Photovolt. Res. Appl. **10**, 55 (2002).

[2] R. B. BERGMANN, C. BERGE, T. J. RINKE, J. SCHMIDT, AND J. H. WERNER, Solar Energy Materials & Solar Cells **74**, 213 (2002).

4.11 Temperature-Dependent Quantum Efficiency Analysis of Recombination Centers in Silicon Thin-Film Solar Cells

Author: T. A. WAGNER
In collaboration with: U. Rau

The minority carrier diffusion length L_D is the primary figure of merit that defines the photovoltaic quality of a semiconductor material. Therefore, the analysis of L_D in solar cells, preferably with the help of internal quantum efficiency (IQE) measurements, belongs to the standard tools of photovoltaic device analysis. In most situations, the recombination centers that determine L_D are not experimentally accessible because of their low concentration. Even if defects in the semiconductor are identified by e.g. Deep Level Transient Spectroscopy (DLTS), identification of these defects as those centers that are relevant for recombination remains a matter of mere correlation. In recent years, lifetime spectroscopy (LS) has emerged as a useful method for the identification of active recombination centers in silicon wafers [1-3].

We introduce temperature-dependent internal quantum efficiency (TQE) measurements as a specific, device-based variant of LS. The devices under investigation are epitaxial thin-film silicon solar cells with a thickness of around 15 μm, grown by ion-assisted deposition (IAD) on highly conductive (100)-oriented Si-substrate wafers at low deposition temperatures of T_{dep} = 460°C. For the TQE measurements, the spectral reflectance and the external quantum efficiency (EQE) of the samples are measured at room temperature (RT) in a conventional setup yielding finally the standard internal quantum efficiency IQE(RT) of each sample as a reference. Subsequently, the samples are mounted into an optical cryostate and the EQE is measured in a range of temperatures T_m between 140 K and 400 K.

Figure 1 shows IQE spectra of an IAD sample in a temperature range T_m = 140 to 380 K. These spectra already indicate that carrier collection is strongly temperature-dependent in this cell. However, the extraction of the minority carrier lifetime τ from IQE spectra requires corrections for the temperature dependence of the absorption coefficient α of Si. Fitting the experimental data to a Shockley-Read-Hall statistics model for the lifetime allows for the determination of the activation energies E_a and reference time constants τ_{n0} (300 K) for the dominant recombination centers. Figure 2 shows Arrhenius plots of the quantity τ/Θ with $\Theta = T_m/300$ K for four IAD samples. In this case, a lifetime model with two

independent defect levels yields activation energies around 70-110 and 160-210 meV for the two dominant recombination centers.

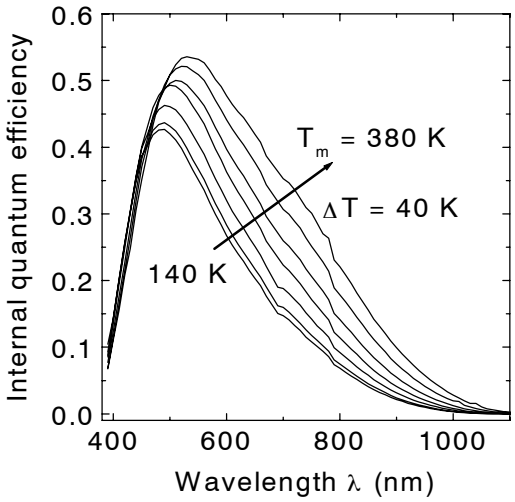

Figure 1: Temperature-dependent internal quantum efficiencies of a thin film solar cell deposited by ion-assited deposition for measurement temperatures T_m between 140K and 380K.

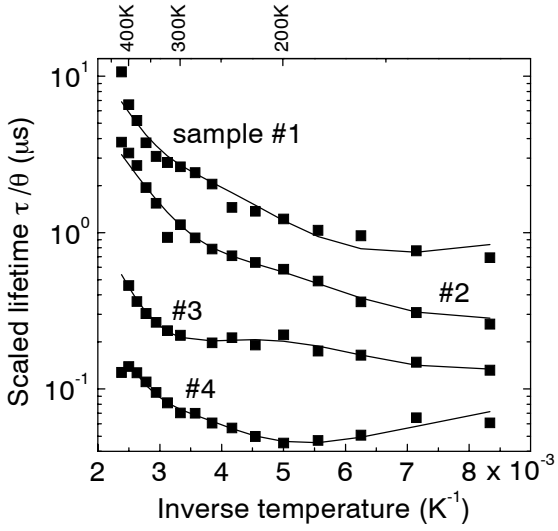

Figure 2: Arrhenius plots of the scaled lifetimes τ/Θ obtained from temperature-dependent quantum efficiency (TQE) measurements on IAD-grown silicon thin film solar cells. The scaling factor is $\Theta=T_m/300K$ where T_m denotes the temperature of the measurement.

We find clear thermally activated features in all IAD thin-film cells investigated. However, for some devices difficulties arise because, within the necessary temperature range, L_D either exceeds the thickness d of the photovoltaicly active base or falls below the width w of the space charge region. In both cases the extraction of the *bulk* diffusion length L_D from IQE spectra becomes difficult or even ambiguous. Within the restriction $d \geq L_D \geq w$, however, TQE analysis of completed solar cells proves to be a reliable device-based method for detecting and analyzing recombination centers that limit the diffusion length and, in consequence, the photovoltaic performance of solar cells.

References:

[1] F. SHIMURA, T. OKUI, AND T. KUSAMA, J. Appl. Phys. **67**, 7168 (1990).

[2] Y. KIRINO, A. BUCZKOWSKI, Z. J. RADZIMSKI, G. A. ROZGONYI, AND F. SHIMURA, Appl. Phys. Lett. **57**, 2832 (1990).

[3] S. REIN, T. REHRL, W. WARTA, AND S. W. GLUNZ, J. Appl. Phys. **91**, 2059 (2002).

4.12 Encapsulation of a Retina Implant

Author: M. ROJAHN
In collaboration with: M. B. Schubert, F. Brümmer[1], B. Rehkopf[1], D. Hülser[1], S. Maisch[2], S. Seifritz[2], V. Bucher[3], S. Bauerdick[3]

Over the last years, research groups have started developing semiconductor-based implants for the light-sensitive retina part of the eye. Such devices aim at restoring some vision for blind patients with a certain eye disease pattern [1]. Today´s implanted devices with a SiO_2-encapsulation show pit-corrosion and progressive dissolution of the material after six months in animal tests.

This contribution evaluates three alternative biocompatible materials which are encapsulation candidates for future retina implants: (i) SiO_x:C/SiN_y, (ii) benzocyclobutene (BCB) and (iii) polyimide 2611 (PI). In order to be able to detect early stages of changes at the polymer's surface, a process for the fabrication of ultra-thin samples with a thickness $d_{or} \approx 50$ nm is developed. X-ray photoelectron spectroscopy (XPS) and Fast Fourier infrared spectroscopy (FTIR) serve to analyse the chemical composition of the materials; impedance spectroscopy (IS) observes the electronic behaviour of the dielectrics. In order to partly simulate the in-vivo conditions of implants, in-vitro experiments with tumor cell lines are devised in this contribution. The combined data from all analytical experiments allow a ranking of the materials with regard to their overall biostability:

SiO_x:C/SiN_y reaches third position. Deposited at temperatures below 100 °C, the sandwich structure is biostable over several weeks and impedance spectroscopy points to a low pin-hole density. However, both FTIR and XPS show a decline in the number of Si-N bonds, see Figures (1) and (2). A numerical analysis yields a dissolution rate $dss \approx 1...2$ nm d^{-1} of the top SiN_x layer in cell culture media.

BCB comes on second position. Only a minor decrease of the material specific Si-O-Si ether bonds is observed after the exposure to the cell culture media.

PI 2611 is the most promising material for the long-term protection of the implant: FTIR proves the chemical resistance of the PI backbone

[1] Dept. of Biology, University of Stuttgart
[2] Dept. of Organic Chemistry, University of Stuttgart
[3] Natural and Medical Science Institute at the University of Tübingen (NMI)

structure. Within the first 24 h of exposure to an electrolyte, IS and XPS point to a diffusion-like process of electrolyte components into the surface layer of the polyimide. Based on a physical model of the polyimide layer, this contribution develops an electric equivalent circuit for the PI-electrolyte system in the frequency range $f = 10^{-3}$ ... 10^{7} Hz. The Helmholtz double layer and the bulk material are each described by a parallel RC element; the PI's surface region is represented by a diffusion impedance. The diffusion process leads to an interface region $d_{IF} \approx 3...10$ nm at the PI´s surface, where ions or molecules are embedded into the matrix of the PI. The "water uptake" does not, however, result in the break-up of the chemical backbone structure.

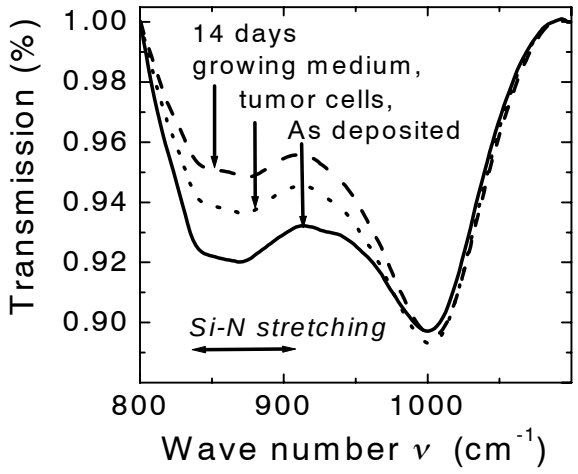

Figure 1: FTIR spectra of SiO_x:C/SiN_y samples for Si-N stretching modes. The increase of the transmission after exposure to growing medium demonstrates the dissolution of the material.

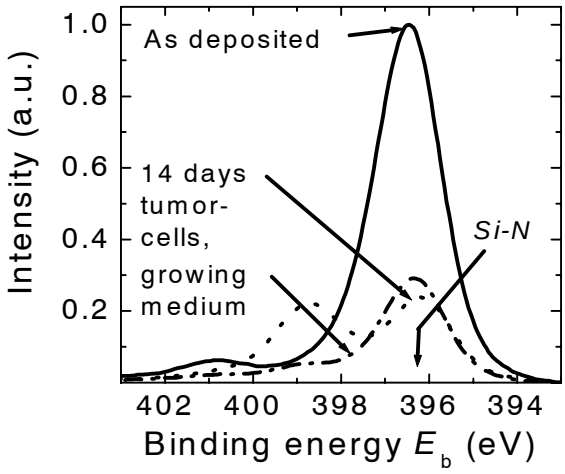

Figure 2: XPS spectra of SiN_x samples. The Si-N peak decreases after cell treatment or exposure to the growing medium, indicating the break-up of Si-N bonds at the SiN_x surface.

Kohler [2] examines with optical microscopes PI- and BCB samples after implantation in laboratory animals for one year. Preliminary results show no degradation of either polymer and a high adhesive strength of the stimulation electrode-PI system, thereby supporting the analytically found superior biostability of the polyimide [2]. PI 2611 will be the encapsulation material of the next generation of subretinal implants.

References:

[1] E. Zrenner, Science **295**, 1022 (2002).

[2] K. Kohler and M. Stelzle, personal communication.

4.13 Position Sensors for Optical Alignment

Author: C. KÖHLER
In collaboration with: B. Lutz, M. B. Schubert

The precise alignment of optical components in high energy physics is a demanding task. Position sensor arrays based on analogue photoconductivity changes in a non-patterned amorphous silicon layer are capable of providing sub-µm spatial resolution when exposed to a probe laser beam of 2-3 mm diameter [1,2]. In practical operation, some tens of such sensors are placed along the propagating laser beam for adjusting measurement equipment over long distances. Hence, such sensors require optical transmission as high as possible.

The overall sensor structure is depicted in figure 1. A glass wafer with a proper anti-reflection coating serves as a substrate. Several thin-film deposition and intermediate patterning steps are needed to form the final sensor array. The readout electronics addresses a 64-rows by 64-columns matrix made up of rectangular zinc oxide (ZnO) stripes as transparent top and bottom contacts to the amorphous silicon (a-Si:H) sensor layer. In order to minimize dark currents, an additional silicon carbide (a-SiC:H) layer is inserted into the layer sequence. The resulting additional a-SiC:H/a-Si:H heterostructure lowers the dark current of the sensor by up to two orders of magnitude. Figure 2 presents a series of typical current/voltage characteristics, in dependence of the incident light intensity.

The thickness of the single layers is optimised for maximum optical transmission at the laser wavelength of 780 nm. Figure 3 demonstrates transmission values in excess of 90% with a good uniformity over the whole 4-inch wafer. The a-Si:H plasma deposition proves to be fairly uniform, whereas sputter deposition of Al-doped ZnO is the limiting process with regards to thickness uniformity.

The single layers are patterned by photolithography. The major requirement for all processing steps is ultimate precision and cleanliness. Due to electrostatic charging of the glass substrate, the contamination by particles, both inside the thin-film deposition systems as well as from the laboratory environment, is the most challenging obstacle on our way to 100% yield and performance.

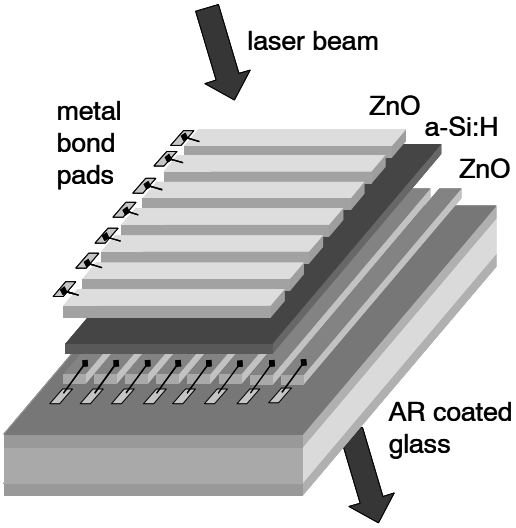

Figure 1: Sketch of the sensor structure. The 64x64 sensor array covers an area of (20x20) mm², with 300 µm wide ZnO stripes at a spacing of 15 µm.

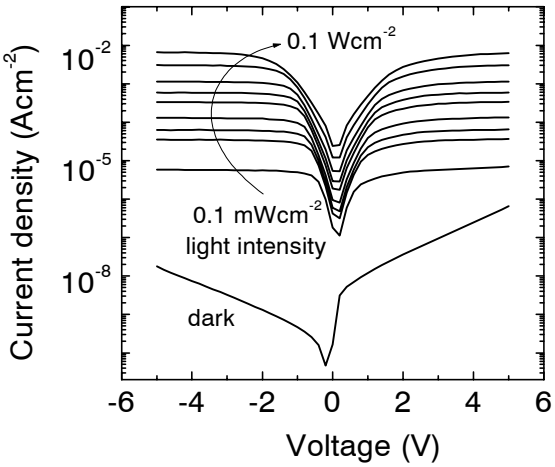

Figure 2: Light-intensity dependence of the current/voltage-characteristics for a large-area test pattern that is used as a process control monitor during sensor manufacturing.

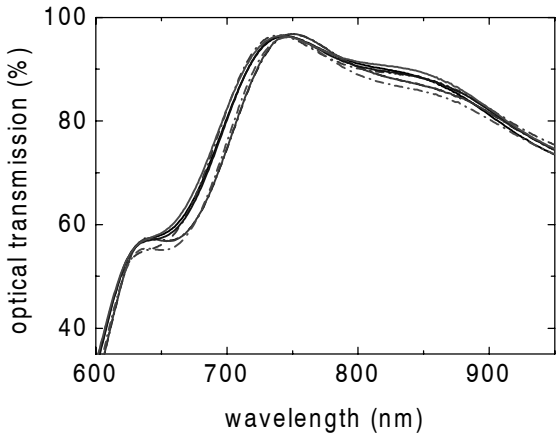

Figure 3: The optical transmisson of test samples reaches far above 90%. The different curves taken at different locations on the same 4-inch wafer prove the homogenity of the deposition. Proper tuning of the thickness of the single layers allows for shifting the transmission maximum to accommodate the desired operating wavelength of the positioning laser.

Ongoing work develops a similar sensor, comprising a larger area of 30x30 mm², and an operating laser wavelength of 670 nm.

References:

[1] V. BARTHELD, *Entwicklung eines optischen Positionsüberwachungssystems höchster Präzision für das Myonspektrometer des ATLAS-Detektors am CERN* (DIPLOMARBEIT TU MÜNCHEN, 1997).

[2] F. BAUER, M. FERNANDEZ GARCIA, S. HORVAT, H. KROHA, A. OSTAPCHUK, AND S. SCHAEL, IEEE Trans. Nucl. Sci. **48**, 262 (2001).

5. Verzeichnis der Publikationen/ *List of Publications*

(erschienen 11/2001 bis 10/2002 / published 11/2001 to 10/2002)

1 M. R. BALBOUL, U. RAU, G. BILGER, M. SCHMIDT, H. W. SCHOCK, AND J. H. WERNER, *Control of Secondary Phase Segregations during $CuGaSe_2$ Thin Film Growth*, J. VAC. SCI. TECHN. A **20**, 1247 (2002).

2 M. R. BALBOUL, M. TURCU, I. M. KÖTSCHAU, U. RAU, AND H. W. SCHOCK, *Sodium-induced Phase Segregations in $CuGaSe_2$ and $CuInSe_2$ Thin-films,* in *Proc. 17th Europ. Photov. Solar Energy Conf.*, B. MCNELIS, W. PALZ, H. A. OSSENBRINCK, AND P. HELM, eds. (WIP-Munich, Germany, 2002) p. 1015.

3 C. BERGE, R.B. BERGMANN, T.J. RINKE AND J.H. WERNER, *Monocrystalline Si Thin Film Solar Cells by Layer Transfer,* in *Proc. 17th Europ. Photov. Solar Energy Conf.*, B. MCNELIS, W. PALZ, H. A. OSSENBRINCK, AND P. HELM, EDS. (WIP-Munich, Germany, 2002) p. 1277.

4 R. B. BERGMANN AND J. H. WERNER, *The Future of Crystalline Silicon Thin Films on Foreign Substrates,* Thin Solid Films **403-404**, 162 (2002).

5 R. B. BERGMANN, C. BERGE, T. J. RINKE, J. SCHMIDT, AND J. H. WERNER, *Advances in Monocrystalline Si Thin Film Solar Cells by Layer Transfer,* Solar Energy Materials and Solar Cells **74**, 213 (2002).

6 F. J. HAUG, D. RUDMANN, G. BILGER, H. ZOGG AND A. N. TIWARI, *Comparison of structural and electrical properties of $Cu(In,Ga)Se_2$ for substrate and superstrate solar cells,* Thin Solid Films **403-404**, 293 (2002).

7 N. JENSEN, R. M. HAUSNER, R. B. BERGMANN, J. H. WERNER, AND U. RAU, *Optimization and characterization of amorphous silicon/crystalline silicon heterojunction solar cells*, Prog. Photovolt. Res. Appl. **10**, 1 (2002).

8 S. KRAFT, B. SCHATTAT, W. BOLSE, S. KLAUMÜNZER, F. HARBSMEIER, A. KULINSKA, AND A. LÖFFL, *Ion beam mixing of ZnO/SiO_2 and Sb/Ni/Si interfaces under heavy ion irradiation*, J. Appl. Phys. **91**, 1129 (2002).

9 G. KRON, T. EGERTER, G. NELLES, A. YASUDA, J. H. WERNER, AND U. RAU, *Electrical Characterization of Dye Sensitized Nanocrystalline TiO_2 Solar Cells with Liquid Electrolyte and Solid-State Organic Hole Conductor*, Thin Solid Films **403-404**, 242 (2002).

10 G. KRON, G. NELLES, T. MITEVA, A. YASUDA, J. H. WERNER, AND U. RAU, *Junction Admittance of Dye Sensitized Nanoporous TiO_2 Solar Cells*, in *Meeting Abstracts of the Centennial Meeting of The Electrochemical Society* (The Electrochemical Society, Pennington, NJ, 2002) abstr. no. 1054.

11 TH. MEYER, F. ENGELHARDT, J. PARISI, AND U. RAU, *Spectral Dependence and Hall Effect of Persistent Photoconductivity in Polycrystalline Cu(In,Ga)Se_2 Thin Films*, J. Appl. Phys. **91**, 5093 (2002).

12 M. NERDING, R. DASSOW, S. CHRISTIANSEN, J. R. KÖHLER, J. KRINKE, J. H. WERNER, AND H.-P. STRUNK, *Microstructure of Laser-crystallized Silicon Thin Films on Glass Substrates,* J. Appl. Phys. **91**, 4125 (2002).

13 Q. NGUYEN, U. RAU, M. MAMOR, K. ORGASSA, H. W. SCHOCK, AND J. H. WERNER*, Electrical Metastability in Cu(In,Ga)Se_2–based Solar Cells with $In_x(OH,S)_y$, CdS, and Combined Buffer Layers,* in *Proc. 17th Europ. Photov. Solar Energy Conf.*, B. MCNELIS, W. PALZ, H. A. OSSENBRINCK, AND P. HELM, eds. (WIP-Munich, Germany, 2002) p. 1107.

14 K. ORGASSA, U. RAU, Q. NGUYEN, H. W. SCHOCK, AND J. H. WERNER, *Role of the CdS Buffer Layer as an Active Optical Element in Cu(In,Ga)Se_2 Thin Film Solar Cells*, Prog. Photovolt. Res. Appl. **10** , 457 (2002).

15 K. ORGASSA, Q. NGUYEN, I. M. KÖTSCHAU, U. RAU, H. W. SCHOCK, AND J. H. WERNER, *Optimized Reflection of CdS/ZnO Window Layers in Cu(In,Ga)Se_2 Thin-film Solar Cells*, in *Proc. 17th Europ. Photov. Solar Energy Conf.*, B. MCNELIS, W. PALZ, H. A. OSSENBRINCK, AND P. HELM, eds. (WIP-Munich, Germany, 2002) p. 1039.

16 U. RAU, A. JASENEK, K. WEINERT, H. W. SCHOCK, AND J. H. WERNER*, Device and Defect Physics of Electron-irradiated ZnO/CdS/Cu(In,Ga)Se_2 Heterojunction Solar Cells*, in *Proc. 17th Europ. Photov. Solar Energy Conf.*, B. MCNELIS, W. PALZ, H. A. OSSENBRINCK, AND P. HELM, eds. (WIP-Munich, Germany, 2002) p. 2191.

17 T.J. RINKE, G. HANNA, K. ORGASSA, H.-W. SCHOCK AND J.H. WERNER*, Novel Self-Aligning Series-Interconnection Technology for Thin Film Solar Modules*, in *Proc. 17th Europ. Photov. Solar Energy Conf.*, B. MCNELIS, W. PALZ, H. A. OSSENBRINCK, AND P. HELM, EDS. (WIP-Munich, Germany, 2002) p. 474.

18 D. RUDMANN, F.-J. HAUG, M. KAELIN, H. ZOGG, A. N. TIWARI AND G. BILGER, *Low Temperature Growth of CIGS Thin Films for Flexible Solar Cells,* Mat. Res. Soc. Symp. Proc. **668**, H3.8.1 (2001).

19 G. SAN VICENTE, J. HERRERO, A. MORALES, M. T. GUTIERREZ, M. HARTMANN, A. JASENEK, AND H. W. SCHOCK*, The Application of Metallic Foils as Substrate for CIGS Thin Film Solar Cells*, in *Proc. 17th Europ. Photov. Solar Energy Conf.*, B. MCNELIS, W. PALZ, H. A. OSSENBRINCK, AND P. HELM, EDS. (WIP-Munich, Germany, 2002) p. 1098.

20 J. SCHMIDT, A. CUEVAS, S. REIN, AND S.W. GLUNZ, *Fill Factor Limitations and Non-Ideal Diode Behaviour of Czochralski Silicon Solar Cells Due to Light-Induced Recombination Centres,* in *Proc. 17th Europ. Photov. Solar Energy Conf.*, B. MCNELIS, W. PALZ, H. A. OSSENBRINCK, AND P. HELM, EDS. (WIP-Munich, Germany, 2002) p. 1396.

21 J. SCHMIDT, L. OBERBECK, T. RINKE, C. BERGE AND R. BERGMANN, *Application of Plasma Silicon Nitride to Crystalline Thin-Film Silicon Solar Cells*, in *Proc. 17th Europ. Photov. Solar Energy Conf.*, B. MCNELIS, W. PALZ, H. A. OSSENBRINCK, AND P. HELM, EDS. (WIP-Munich, Germany, 2002) p. 1351.

22 H. W. SCHOCK AND U. RAU, *The Role of Structural Properties and Defects for the Performance of Cu-chalcopyrite-based Thin-film Solar Cells,* Physica B **308-310**, 1081 (2002).

23 M. TURCU, I. M. KÖTSCHAU, AND U. RAU, *Composition Dependence of Defect Energies and Band Alignments in the $Cu(In_{1-x}Ga_x)(S_{1-y}\ S_y)_2$ Alloy System*, J. Appl. Phys. **91**, 1391 (2002).

24 M. TURCU, O. PAKMA, AND U. RAU, *Interdependence of Absorber Composition and Recombination Mechanism in $Cu(In,Ga)(Se,S)_2$ Heterojunction Solar Cells*, Appl. Phys. Lett. **80**, 2598 (2002).

25 T. A. WAGNER, L. OBERBECK, AND R. B. BERGMANN, *Low Temperature Epitaxial Silicon Films Deposited by Ion-assisted Deposition*, Mat. Sci. Eng. B **89**, 319 (2002).

26 R. J. WALTERS, G. P. SUMMERS, S. R. MESSENGER, A. JASENEK, H. W. SCHOCK, U. RAU, J. NOCERINO, J. TRINGE, AND K. REINHARDT, *Displacement Damage Dose Analysis of Proton Irradadiated CIGS Solar Cells on Flexible Substrates*, in *Proc. 17th Europ. Photov. Solar Energy Conf.,* B. MCNELIS, W. PALZ, H. A. OSSENBRINCK, AND P. HELM, eds. (WIP-Munich, Germany, 2002) p. 2191.

27 K. WEINERT, U. RAU, A. JASENEK, H. W. SCHOCK, J. H. WERNER, M. YAKUSHEV, B. SCHATTAT, AND W. BOLSE, *Analysis and Modelling of Electron and Proton Irradiation Damage in $Cu(In,Ga)Se_2$ solar cells*, in *Proc. 17th Europ. Photov. Solar Energy Conf.*, B. MCNELIS, W. PALZ, H. A. OSSENBRINCK, AND P. HELM, eds. (WIP-Munich, Germany, 2002) p. 2167.

6 Promotionen 2002 / *Ph. D. Theses 2002*

BRÜHNE, KAI	Hot-Wire Gasphasenabscheidung von nanokristallinem Silicium und Silicium-Germanium
JASENEK, AXEL	Eigenschaften von Defekten in Cu(In,Ga)Se_2 nach Elektronen- und Protonenbestrahlung
KOCH, CHRISTIAN	Niedertemperaturabscheidung von Dünnschicht-Silicium für Solarzellen auf Kunststofffolien
QUINTUS, MARTIN	Kompositelektroden und –membranen für Polymerelektrolytmembranbrennstoffzellen
SCHMIDT, MARION	Prozeßtoleranz und Stabilität von Cu(In,Ga)Se_2-Solarzellen

7 Diplomarbeiten 2002 / *Diploma Theses 2002*

BÄDER, DANIEL	Charakterisierung von Dünnschichtsolarzellen mit elektronenstrahlinduzierten Strömen im Rasterelektronenmikroskop
BRENDLE, WILLI	Influence of Copper on the Carrier Lifetime in Silicon
CABIR, YUSUF	Robuste Fahrzeugerkennung mit CMOS-Kameras
DE SOUZA, PAULA	Flexible Cu(In,Ga)Se_2-Solarzellen: Wechselwirkung zwischen Substrat und Absorberschicht
KLEINSASSER, JOCHEN	Messung und Analyse der Leistungsdaten von Positionssensoren
MATTHEIS, JULIAN	Transporteigenschaften von a-Si:H/c-Si Heterostruktur-Solarzellen
PUZIC, ALEKSANDAR	Untersuchung zur Spindynamik in nanostrukturierten ferromagnetischen Schichtsystemen

8 Studienarbeiten 2002 / *Student Works 2002*

BAYER, ROLF	Praktikumsversuch „Laserdioden“
ELSER, DOMINIQUE	Laserannealing von Cu(In,Ga)Se_2-Schichten
HLUSIAK, MARKUS	Streuende Fensterschichten für Cu(In,Ga)Se_2-Solarzellen
ROSTAN, JOHANNES	Spectral dependence of the photoconductance and the open-circuit voltage of bifacial silicon solar cell precursors
SCHLEUSSNER, SEBASTIAN	Wachstum hocheffizienter Cu(In,Ga)Se_2-Absorberschichten in Abhängigkeit von Natrium und Selen

9 *ipe* Kolloquium 2002

07.01. THOMAS HAHN, Universität Jena, *"Epitaxie von Chalcopyrithalbleitern auf Si"*
21.01. RALF KÖNENKAMP, Hahn-Meitner-Institut, Berlin, *"Solarzellen mit extrem dünnem Absorber"*
28.01. DAVID CAHEN, Weizmann Institute, Rehovot, Israel, *"Molecule-controlled electronic devices: Separating electron transport from molecules"*
04.02. HEINRICH BECKER, Covion, Frankfurt/Main, *"Organische Halbleiter: Keine Angst vor großen Molekülen!"*
15.04. MARTIN HOHEISEL, Siemens AG Medical Solutions, , *"Anforderungen an amorphe Halbleiter für medizinische Röntgendetektoren"*
22.04. MELANIE NERDING, Universität Erlangen-Nürnberg, *"Textur und Korngefüge laserkristallisierter Siliziumfilme"*
29.04. JÜRGEN KÖHLER, Universität Stuttgart, ipe, *"Sicherheit im Umgang mit Lasern"*
06.05. JOHANN SPRINGER, Zentrum für Sonnenenergie- und Wasserstoff-Forschung, Stuttgart, *"Verkapselung von CIS-Solarmodulen - Standard und Alternativen"*
13.05. ADOLF GIESSEN, Universität Stuttgart, IFSW, *"Hochleistungsscheibenlaser"*
03.06. GÜNTER REITEMANN, Universität Stuttgart , IHT, *"Excess current investigations of silicon p^+-i-n^+ diodes"*
10.06. KRISTIAN PETER, Universität Konstanz, *" Dünnschichtsolarzellen"*
17.06. STEFAN GLUNZ, Fraunhofer ISE, Freiburg, *"Monokristalline Siliziumsolarzellen: Materialanalyse und Zellstrukturentwicklung am Fraunhofer ISE"*
24.06. RÜDIGER BUSS, Universität Duisburg, *"Einsatz optoelektronischer Technologien in implantierbaren Mikrosystemen"*
01.07. NORBERT NICOLOSO, DLR Stuttgart, *"Carbon nanotube/ (Pt, Ru) electro catalyst for fuel cells "*
08.07. FRANZ KARG, Shell Solar, München, *" Dünnschichtsolarzellen"*
14.10. RALF BERGMANN, Robert Bosch GmbH, Schillerhöhe, *" Forschung und Vorausentwicklung in der Robert Bosch GmbH am Beispiel der Abteilung "Angewandte Physik" "*
28.10. KURT TARETTO, Universität Stuttgart, ipe, *"Diskussion zur Herleitung der Solarzellenkennlinie"*
11.11. THOMAS SCHLENKER, Universität Stuttgart, ipe, *"Wachstumsexperimente von CIGS auf Mo-Substraten"*
18.11. AINHOA ESTURO-BRETON, Universität Stuttgart, ipe, *"Laserdotierung von Si-Solarzellenemittern"*
25.11. MARTIN WAGNER, Universität Stuttgart, ipe, *"Astrophotographie"*
09.12. NGUYEN QUANG, Universität Stuttgart, ipe, *" Heterointerfaces in Cu(In,Ga)Se2 solar cells"*
16.12. MIRCEA TURCU, Universität Stuttgart, ipe, *" Electronic properties of wide-gap Cu(In,Ga)(Se,S)$_2$ chalcopyrites "*

10 Gäste und Stipendiaten 2002 / *Guests 2002*

CAO XINMIN , Research Center for Electric Light Sources, Southeast University, Nanjing, VR China, 1.10.1999 – 15.9.2002

DE SOUZA PAULA, Institut de Sciences de la Matière et du Rayonnement, École Nationale Superieure d'Ingénieurs ISMRA-ENSI Caen, Frankreich, 19.03.2002 – 19.09.2002

ESTURO-BRETÓN AINHOA, UPV-Universidad del Pais Vasco, Spanien, 01.12.2001 – 30.09.2005

LOURO-ANTUNES PAULA, Institut Superior de Engenharia de Lisboa (ISEL), Portugal, August 2002

NGUYEN HONG QUANG, National Center for Natural Science and Technology, Hanoi, Vietnam, 1.10.1999 – 30.09.2003

NGUYEN XUAN VIET, National Center for Natural Science and Technobgy, Hanoi, Vietnam, 1.11.2001 – 30.09.2004

SHEN DASHEN, Dept. of Electrical and Computer Engineering, University of Alabama, Huntsville, USA, 15.10.2002 – 05.12.2002

YI MAOXIANG, Hefei University of Technology, Baoding, China, 01.10.02 – 30.09.03

11 Wissenschaftliche Geräte und Analysemethoden / *Scientific Instruments and Methods of Analysis*

11.1 Abscheideverfahren */ Deposition Methods*

Material / *Materials*	**Abscheideverfahren / *Deposition method***	**Anwendung / *Application***	**Kontakt / *Contact***
Amorphe Halbleiter / *amorphous semiconductors* (a-Si:H, nc-Si, etc.)	Plasma-CVD (DC, RF, VHF), Niedertemperatur (70°C)/ *low temp. deposition (70°C)* thermokatalytische Depos. *hot-wire-CVD* Legierung / *alloying* (Ge, C) Dotierung / *doping* (B,P,..)	Dünnschicht-Solarzellen und Sensoren / *thin-film solar cells and sensors*	Schubert
Kristallines Silicium / *crystalline silicon* (mono, poly-Si)	CVD, RT-CVD,Plasma-CVD Hot-wire- CVD Ionenassistierte Epitaxie / *Ion Assisted Deposition (IAD)*	Dünnschicht-Solarzellen und Elektronik / *thin-film solar cells and electronics*	Schubert
Kristallines Silicium / *crystalline silicon*	Laserkristallisation / *laser crystallization*	Dünnschicht-transistoren / *thin-film transistors*	Köhler
Poröses Silicium / *porous silicon*	Transferverfahren / *transfer methods*	Elektronik auf Glas und flexiblen Sustraten / *Electronics on glass and flexible substrates*	Schubert
Polykristalline Verbindungs-halbleiter / *compound semiconductors* $Cu(In,Ga)(Se,S)_2$ CdS,ZnS, ZnSe,	Aufdampfung, mit mehreren Quellen und individueller Ratenregelung, Katodenzerstäubung, chemische Badabscheidung / *multi-source evaporation*, *sputtering, chemical bath deposition*	Dünnschicht-Solarzellen / *thin-film solar cells*	Schock
Transparente leitfähige Schichten / *transparent conducting films* ITO, ZnO, SnO_2	Katodenzerstäubung / *sputtering (RF, DC, reactive)*	Solarzellen und Sensoren / *solar cells and sensors*	Schock, Schubert

11.2 Strukturelle Analysenverfahren */ Structural Materials Analysis*

Methode / *Method*	**Material / *Materials***	**Anwendung / *Application***	**Kontakt / *Contact***
Photoelektronen-spektroskopie / *photoelectron spectroscopy (small spot XPS/-ESCA, UPS)*	Halbleiter Oberflächen, Dünnschichten / *semiconductor surfaces, thin-films* $CuInSe_2$, ZnO	Solarzellen (in-situ Studien des Wachstums, elektronische Bandstruktur) / *solar cell materials (growth, band structure)*	Bilger
Sekundär-Ionen Massenspektro-metrie / *Secondary Ion Mass Sectroscopy (SIMS)*	Dünne Schichten, Schichtsysteme / *compositional analysis of thin films*	Laterale Elementverteilungen, Tiefenprofile, Spurenelemente / *lateral element distribution, depth profiles, trace elements*	Bilger
Diffraktometrie (streifender Einfall) / *grazing incidence X-ray diffraction*	Silizium-, Verbindungshalbleiter-schichten / *thin film silicon and compound semiconductors*	Phasenanalyse, Textur von dünnen Schichten / *phase analysis,texture of thin films*	Schock
Rasterelektronen-mikroskopie (incl. Röntgenanalyse) / *scanning electron microscopy, energy dispersive x-ray analysis*	Mikro- und polykristalline Dünnschichten / *micro- and polycrystalline thin films*	Struktur, chemische Zusammensetzung, Tiefenprofile / *structure, chemical composition, depth profiling*	Schock
Rasterkraft- und Rastertunnelmi-kroskopie / *atomic force and scanning tunneling microscopy*	Oberflächen von mikro- und polykristallinen Dünnschichten / *Surfaces of micro- and polycrystalline thin films*	Elektrische und strukturelle Eigenschaften von Halbleiteroberflächen / *semiconductor surfaces (electronic and structural properties)*	Schock

11.3 Analyse optischer Eigenschaften/ *Analysis of Optical Properties*

Methode / *Method*	**Material**	**Anwendung / *Application***	**Kontakt / *Contact***
FT-IR-Spektroskopie / *FT-IR-spectroscopy*	wasserstoffhaltige, amorphe und mikrokristalline Dünnschichthalbleiter / *hydrogen-containing amorphous and microcristalline thin film semiconductors*	Solarzellen, Sensoren (Wasserstoffgehalt, strukturelle Eigenschaften) / *solar cells, sensors*	Schubert
Raman-Spektroskopie / *Raman-spectroscopy*	amorphe und mikrokristalline dünne Schichten / *amorphous and microcrystalline thin films*	Solarzellen, Sensoren (strukturelle Eigenschaften) / *solar cells, sensors*	Schubert
Photolumineszenz / *photoluminescence*	Silizium, Verbindungs-halbleiter / *silicon, compound semiconductors*	Charakterisierung von Halbleitern / *characterization of semiconductors*	Rau
Photothermische Ablenkungs-Spektroskopie / *photothermal deflection spectroscopy* (PDS) Methode des konst. Photostroms./. *Constant Photocurr. method (CPM)*	dünne Schichten / *thin films*	optische von Absorption Halbleiterschichten / *optical absorption of semiconductor thin films*	Schubert
Transmission, Reflexion / *optical transmission and reflection (UV to NIR, direct, diffuse)*	dünne Schichten für Solarzellen, Sensorik und Optoelektronik / *thin films for solar cells, sensors, and opto-electronics*	Bestimmung von Schichtdicke, Brechungsindex, Extinktionskoeffizient / *film thickness, refractive index, absorption* .	Rau
In-situ Ellipsometrie / *in-situ ellipsometry*	dünne Schichten, Mehrschichtsysteme / *thin films, multi-layer systems*	Schichtwachstum und Grenzflächeneffekte / *film growth*	Schubert

11.4 Analyse elektro-optischer Eigenschaften / *Analysis of Electro-Optical Properties*

Methode / *Method*	**Material / *Materials***	**Anwendung / *Application***	**Kontakt / *Contact***
Stationäre und transiente Photo- und Dunkel-leitfähigkeit / *stationary and transient dark- and photoconductance*	amorphe und polykristalline Dünnschichthalbleiter / *amorphous and polycrystalline thin-film semiconductors*	Bestimmung von Trägerdichten, Diffusionslängen, Fermi-Energie / *carrier densities, diffusion lengths, Fermi energy, etc*.	Schubert
Hall Messungen, Time-Of-Flight Spektroskopie, Quantenausbeute, transiente Mikrowellen-absorption / *Hall measurements, Time-Of-Flight (TOF) spectros-copy, quantum efficiency, μ-wave absorption*	Halbleitermaterialien und -baulelemente / *semiconductor materials and devices*	Trägerbeweglichkeiten, Diffusionslängen, Minoritätsträger-lebensdauer, elektro-nische Zustandsdichte / *carrier mobilities, diffusion lengths, minority carrier lifetime, densities of states*	Rau
Admittanz-Spektroskopie, DLTS, modulierte Photoströme / *admittance, DLTS, modulated photocurrents*	Dünnschichthalbleiter und –bauelemente / *thin-film semiconductors and devices*	Solarzellen, Sensoren (Defekte, elektrische Transporteigenschaften , interne Barrieren) / *solar cells, sensors (defects, electronic transport, internal barriers)*	Rau
IU-Kennlinien / *IV characteristics*	Dioden, Solarzellen / *diodes, solar cells*	Transporteigensch. / *transport properties*	Rau
Spektrale Empfindlichkeit, Quantenwirkungs-grad / *Spectral response Quantum-efficiency*	Dioden, Solarzellen / *diodes, solar cells*	Transporteigenschaften optische Eigenschaften / *transport properties optical properties*	Rau

12 Mitarbeiter / *Staff Members*

Name	**Titel**	**Tel.** 0711-685-...	**E-Mail** ...@ipe.uni-stuttgart.de	**Arbeitsgebiet**
ALBERTS, LUKAS	Dr.-Ing.	7142	lukas.alberts	Abscheidungen von amorphem Silicium bei tiefen Temperaturen
BAUER, LEO		7182	leo.bauer	Metallisierung, Photoarbeiten, Maskentechnik
BERGE, CHRISTOPHER	Dipl.-Phys.	7162	christopher.berge	Dünnschicht-Solarzellen aus kristallinem Silicium
BILGER, GERHARD	Dr.-Ing.	7176, 7154	gerhard.bilger	Oberflächenanalytik mit SIMS und XPS; Technologie-Support
BRENDLE, WILLI	Dipl.-Ing.	7178	willi.brendle	Niedertemperaturpassivierung für Transfer-Solarzellen
BRENNER, KLAUS	Dipl.-Ing. (FH)	7201	klaus.brenner	Technologische Infrastruktur und Prozesse der Si-Technologie
CARLSSON, ANNE		7201	anne.carlsson	Prozesse der a-Si-Technologie, Entwicklung einer Ätzzelle
CRAFF CASTILLO, CECILIA	Dipl.-Phys.	7160	cecilia.craff	Rapid Thermal CVD, epitaktisch hergestellte p-n-Übergänge
DEMIR, JAKOB	Dipl.-Ing.	7169	jakob.demir	Herstellung und Charakterisierung von Dünnschichttransistoren
DIEGEL, LYDIA		7163	lydia.diegel	Verwaltung
DOLCH, THOMAS		7182	thomas.dolch	Sputtern von TCO-Schichten, Elektrik, Elektronik
ESTURO-BRETON, AINHOA		7169	ainhoa.esturo-breton	Laserprozessierung von Silicium Solarzellen
GEBHARDT, KERSTIN	Dr. rer. nat.	7142	kerstin.gebhardt	Oberflächenanalytik mit XPS, Heterostrukturen
GEMMER, CHRISTIAN	Dipl.-Phys.	7198	christian.gemmer	Gestapelte Solarzellen aus amorphem und nanokristallinem Silicium
GRABITZ, PETER	Dipl.-Phys.	7197	peter.grabitz	Flexible Verbindungshalbleiter-Solarzellen
HANNA, GEORGE	Dipl.-Phys.	7171	george.hanna	Hochleistungs-Cu(In,Ga)Se_2-Solarzellen, Abscheidung und Analyse von CIGS
JACKSON, PHILIP	Dipl.-Phys.	7198	philip.jackson	Flexible Substrate
KESSLER, ISABEL	M. A.	7141	isabel.kessler	Sekretariat, Verwaltung
KÖHLER, CHRISTIANE	Dipl.-Phys.	7182	christiane.koehler	Si-Niedertemperaturtechnologie, XRD, transparente Kontakte, Ramanstreuung
KÖHLER, JÜRGEN	Dr.-Ing.	7159	juergen.koehler	Laser Annealing, Verwaltung

KRON, GREGOR	Dipl.-Phys.	7160	gregor.kron	Farbstoff-sensibilisierte TiO_2 Solarzellen
KÜHNLE, DENNIS		7200	dennis.kuehnle	Aufdampfen von Halbleiterschichten
LAPTEV, VIKTOR	Dr. rer.nat.	7197	viktor.laptev	Chemische Schichtabscheidung, Röntgenbeugungsmessungen
LOPEZ, LUIS	Dipl.-Ing.	7168	luis.lopez	Information Technology Online und Self-Study-Online
LUTZ, BRIGITTE		7200	brigitte.lutz	Analytik, Elektrochemie, GCMS
MATTHEIS, JULIAN	Dipl.-Ing.	7161	julian.mattheis	Optische Eigenschaften von Solarzellen
NGUYEN HONG QUANG	M.Sc.	7171	quang.nguyen	Oberflächenchemie von Cu(In,Ga)Se_2 , Pufferschichten
NGUYEN XUAN VIET	M. Sc.	7179	viet.nguyen	a.Si:H/c-Si Heterostrukturen
ORGASSA, KAY	Dipl.-Phys.	7181	kay.orgassa	Optische Optimierung von CIGS-Solarzellen
PFISTERER, FRITZ	Dr.-Ing.	7157	fritz.pfisterer	Organisation / Verwaltung / allgemeine Aufgaben / Lehre (Optoelektronik I)
RAKHLIN, MICHAIL	Dipl.-Phys.	7183	michail.rakhlin	Thermoelektrik, Silizium-Germanium-Dünnschichten
RAU, UWE	Dr. rer. nat. habil.	7199	uwe.rau	Elektrische Charakterisierung und Modellierung von Dünnschichtsolarzellen (CIGS, Si, org.)
RIß, ANTON		7214	anton.riss	Werkstatt
ROJAHN, MARTIN	Dipl.-Phys.	7179	martin.rojahn	Herstellung und Verkapselung von Mikro-Photodioden aus a-Si:H
SCHLENKER, THOMAS	Dipl.-Phys.	7178	thomas.schlenker	Wachstum dünner CIGS Absorberschichten
SCHOCK, HANS-WERNER	Dr.-Ing.	7180	hans-werner.schock	Dünnschichttechnik, Photovoltaik-Dünnschichtsolarzellen aus Verbindungshalbleitern
SCHUBERT, MARKUS	Dr.-Ing.	7145	markus.schubert	Projektleitung amorphes und nanokristallines Si, Solarzellen mit Sensoren, Studien- und Diplomarbeiten, www.
STEMPFLE, ULI	Dipl.-Phys.	7170	uli.stempfle	Flexible CIS-Solarzellen
TARETTO-ZEYEN, KURT	Dipl.-Ing.	7181	kurt.taretto	Simulation und elektrische Charakterisierung von Halbleitern
TURCU, MIRCEA	M. Sc.	7184	mircea.turcu	Strukturelle und optische Eigenschaften von Cu(In,Ga)Se_2
V. REKOWSKI, CHRISTINE	M. A.	7141	christine.rekowski	Sekretariat, Verwaltung

WAGNER, MARTIN	Dipl.-Phys.	7184	martin.wagner	Dünnschichtprozesse
WAGNER, THOMAS	Dipl.-Phys.	7161	thomas.wagner	Defektanalyse an Silicium-Niedertemperaturepitaxie-Schichten
WEINERT, KRISTIN	Dipl.-Phys.	7170	kristin.weinert	Elektrische und optische Charakterisierung von CIGS-Solarzellen
WERNER, JÜRGEN	Prof. Dr. rer. nat. habil.	7140	juergen.werner	Institutsleitung
WIESNER, HOLM	Dipl.-Ing.	7197	holm.wiesner	CIS-Technologie
WILLE, WERNER		7158	werner.wille	Buchhaltung, Verwaltung
YI, MAOXIANG		7142	maoxiang.yi	Dünnschichtsolarzellen

13 Lageplan / *Site Plan*